Atmos. Chem. Phys., 12, 1923–1950, 2012
www.atmos-chem-phys.net/12/1923/2012/
doi:10.5194/acp-12-1923-2012

Atmospheric Chemistry and Physics

Coupling processes and exchange of energy and reactive and non-reactive trace gases at a forest site – results of the EGER experiment

T. Foken[1,5], F. X. Meixner[2,4], E. Falge[2], C. Zetzsch[3,5], A. Serafimovich[1,5], A. Bargsten[2], T. Behrendt[2], T. Biermann[1], C. Breuninger[2], S. Dix[1,*], T. Gerken[1], M. Hunner[1,*], L. Lehmann-Pape[2], K. Hens[2], G. Jocher[1,], J. Kesselmeier[2], J. Lüers[1,5], J.-C. Mayer[2], A. Moravek[2], D. Plake[2], M. Riederer[1], F. Rütz[1], M. Scheibe[2,***], L. Siebicke[1,****], M. Sörgel[3], K. Staudt[1,*****], I. Trebs[2], A. Tsokankunku[2], M. Welling[2], V. Wolff[2,*****], and Z. Zhu[2,******]**

[1]University of Bayreuth, Department of Micrometeorology, 95440 Bayreuth, Germany
[2]Max-Planck-Institute of Chemistry, Biogeochemistry Department, P.O. Box 3060, 55020 Mainz, Germany
[3]University of Bayreuth, Atmospheric Chemistry Research Laboratory, 95440 Bayreuth, Germany
[4]University of Zimbabwe, Department of Physics, P.O. Box MP 167, Mount Pleasant, Harare, Zimbabwe
[5]Member of Bayreuth Center of Ecology and Environmental Research (BayCEER), University of Bayreuth, 95440 Bayreuth, Germany
[*]now at: TÜV Süd Industrie Service GmbH Wind Cert Services, Ludwig-Eckert-Straße 10, 93049 Regensburg, Germany
[**]now at: Alfred-Wegener Institute for Polar and Marine Research, Telegrafenberg A43, 14473 Potsdam, Germany
[***]now at: German Aerospace Center (DLR), Institute of Atmospheric Physics, Münchner Straße 20, 82234 Oberpfaffenhofen-Wessling, Germany
[****]now at: Institut National de la Recherche Agronomique (INRA), BP 709, 97387 Cedex Kourou, French Guiana
[*****]now at: Agroscope ART Research Station, Reckenholzstrasse 191, 8046 Zürich, Switzerland
[******]now at: Institute for Geographic Sciences and Natural Resources Research, ChineseAcademy of Sciences (CAS), A11 Datun Road, Anwai, Beijing 100101, China

Correspondence to: T. Foken (thomas.foken@uni-bayreuth.de)

Received: 10 July 2011 – Published in Atmos. Chem. Phys. Discuss.: 21 September 2011
Revised: 9 February 2012 – Accepted: 9 February 2012 – Published: 17 February 2012

Abstract. To investigate the energy, matter and reactive and non-reactive trace gas exchange between the atmosphere and a spruce forest in the German mountain region, two intensive measuring periods were conducted at the FLUXNET site DE-Bay (*Waldstein-Weidenbrunnen*) in September/October 2007 and June/July 2008. They were part of the project "ExchanGE processes in mountainous Regions" (EGER). Beyond a brief description of the experiment, the main focus of the paper concerns the coupling between the trunk space, the canopy and the above-canopy atmosphere. Therefore, relevant coherent structures were analyzed for different in- and above canopy layers, coupling between layers was classified according to already published procedures, and gradients and fluxes of meteorological quantities as well as concentrations of non-reactive and reactive trace compounds have been sorted along the coupling classes. Only in the case of a fully coupled system, it could be shown, that fluxes measured above the canopy are related to gradients between the canopy and the above-canopy atmosphere. Temporal changes of concentration differences between top of canopy and the forest floor, particularly those of reactive trace gases (NO, NO_2, O_3, and HONO) could only be interpreted on the basis of the coupling stage. Consequently, only concurrent and vertically resolved measurements of micrometeorological (turbulence) quantities and fluxes (gradients) of trace compounds will lead to a better understanding of the forest-atmosphere interaction.

Published by Copernicus Publications on behalf of the European Geosciences Union.

1 Introduction

The scientific focus on forest ecosystems has long been the privilege of more than the ecologist. The forest is also a real challenge for micrometeorologists and atmospheric chemists. In the book by Hutchinson and Hicks (1985) the very complex character of the exchange processes between the atmosphere and the forest was highlighted and some of the specific problems like counter-gradients and their consequences were made public for a larger community (Denmead and Bradley, 1985). Other issues, like the roughness sublayer have also been considered (Garratt, 1978, 1980). For a better understanding of the forest atmosphere interaction, the mixing layer hypothesis became an important contribution (Finnigan, 2000; Raupach et al., 1996) and recently a common theory for the roughness sublayer and the mixing layer turned out to be possible (Harman and Finnigan, 2007, 2008). The approach by the mixing layer theory is closely connected with coherent structures (Collineau and Brunet, 1993a, b; Katul et al., 1997) which generate typical ramp structures in the time series of scalar quantities measured above a forest. Such ramp structures (caused by Kelvin-Helmholtz instabilities due to extreme sheering above the top of the aerodynamically rough forest) have also be found in trace gas fluctuations (Rummel et al., 2002).

While for the measurement of turbulent fluxes of momentum, sensible heat, water vapour and carbon dioxide the fast response and direct eddy-covariance technique is state-of-the-art, slow response flux measuring techniques had be applied for most trace gases and aerosol particles, like the aerodynamic method (Arya, 2001; Monteith and Unsworth, 2008) or the modified Bowen-ratio method (Businger, 1986). During the last decade, however, the eddy-covariance technique has become applicable for aerosol particles and a selected number of trace gases – particularly, nitrous oxide (N_2O), methane (CH_4), ozone (O_3), nitric oxide (NO) and nitrogen dioxide (NO_2) (e.g. Rummel et al., 2002; Güsten and Heinrich, 1996; Horii et al., 2004; Pryor et al., 2007; Griffith et al., 2002).

Concepts of micrometeorological measurements, focusing on the exchange of energy and carbon dioxide in and above tall vegetation, have already been formulated in such a way that related phenomena like advection (Aubinet et al., 2003; Lee, 1998), roughness sublayer and mixing layers (Finnigan, 2000; Raupach et al., 1996), as well as coherent structures (Collineau and Brunet, 1993a, b) could be detected. However, better understanding of turbulence structures in and above forest canopies require the investigation of coherent structures in greater detail. Furthermore, as shown by Raupach (1981) and Bergström and Högström (1989), coherent events of low frequency contribute significantly to the budgets of momentum, heat and trace substances in and above forest canopies. Furthermore, low level jets have a significant influence on the night-time exchange of a forest. Karipot et al. (2008, 2006) found that they enhance turbulence and mixing close to the ground due to increased shear.

Therefore, the primary focus of our field studies was the contribution of coherent structures to the transfer of energy, carbon dioxide (CO_2), water vapour (H_2O), and reactive trace compounds (nitric oxide (NO), nitrogen dioxide (NO_2), ozone (O_3), nitrous and nitric acid (HONO and HNO_3), ammonia (NH_3), and related aerosol compounds). Our previous investigations on atmosphere-forest ecosystem coupling have been based on the mixing layer theory, and our first approach defined coupling in relation to characteristic length scales of the distance between coherent eddies and the wind shearing (Wichura et al., 2004; Wichura, 2009). Later, a wavelet transform based technique (Thomas and Foken, 2005, 2007b) has been used. There, the mean temporal scales of coherent structures were estimated via the fitting of a normal Gaussian distribution function to the probability density function of the results from the individual 30-min intervals. Thomas et al. (2006) extended this research by investigation of the boundary layer structure over the forest with particular emphasis on coherent structures.

The ability of forest canopies to absorb trace gases, which are biogenic emitted by plants and/or by the soil below, became known to be an important aspect of atmospheric budgets of trace substances (cf. Ganzeveld et al., 2002). Generally, the amount of absorbed/escaping trace gases is controlled (a) by physiological and/or surface characteristics of forest vegetation and soils, and (b) by the interaction of turbulent transport (in and above canopy) with processes of the gas exchange itself as well as with atmospheric transformations of chemically reactive trace compounds. This is particularly valid for reactive nitrogen and carbon species and, as shown very recently, also for related compounds like radicals and peroxides (e.g. Karl et al., 2010; Farmer and Cohen, 2008; Wolfe et al., 2011a, b). This issue can be focused on the question of coupling, namely how strongly is the entire forest atmosphere (or parts of it) coupled to (or de-coupled from) the surface layer above the canopy. This has substantial consequences for the mean residence time (hence, the in-canopy recycling) of trace compounds (cf. Aubinet et al., 2003; Meixner et al., 2003). Low coupling (de-coupled) situations, resulting in longer residence times, generally favor the efficiency of reactions and transformations between chemically reactive trace gases (e.g. triads of NO-NO_2-O_3 and HNO_3-NH_3-$NH_4NO_{3,\mathrm{aerosol}}$). The constraint on the temporal scales to be considered originates from the Damköhler number (Damköhler, 1940), a ratio of two particular time scales, namely the characteristic turbulent transport time over the characteristic chemical reaction time. For the investigation of in-canopy storage, canopy cycling, and whole ecosystem exchange of reactive trace gases, measurements of vertical profiles of concentrations and fluxes are essential. While methodologies to measure vertical concentration profiles for NO, NO_2, O_3, NH_3, HONO, HNO_3 (NH_4^+, NO_3^-) are state-of-the-art (cf. Trebs et al., 2004), flux

measurements of these compounds by the eddy covariance technique have been (and still are) hampered by the unavailability of fast and specific chemical sensors. However, Rummel et al. (2002) have demonstrated operational eddy covariance flux measurements of NO by applying a specific and fast chemiluminescence analyzers. Horii et al. (2004) applied operational eddy covariance flux measurements of NO and NO_x over a temperate deciduous forest.

In order to elucidate formation pathways of HONO, an important precursor of OH radicals in the lower troposphere, we included in- and above canopy measurements of HONO mixing ratios in our study since the canopy space constitutes a large surface for heterogeneous reactions. Shading may result in different source and sink strengths above and below canopy which are expected to be mirrored in concentration differences. These were analysed with respect to the coupling of the forest and the air layer above the forest by coherent structures.

Furthermore, we included in this study a comparison of two forest models with different closure techniques, the 1st order K-approach and a higher order closure: the 1-D canopy-surface layer model (ACASA, Pyles et al., 2000) and the 3-D model STANDFLUX with a nested structure (STANDFLUX, Falge et al., 1997, 2000). The application of a higher order closure model like ACASA is necessary to overcome the counter-gradient problem and also to model the probable influence of coherent structures.

Against this background the authors joined forces to study diel cycles of energy, water, non-reactive and reactive trace compounds in the soil-vegetation-boundary layer-system. In the frame of a larger project "ExchanGE processes in mountainous Regions (EGER)", joint field experiments focusing the micrometeorology and the behaviour of trace compounds of a spruce-forest have been performed at the FLUXNET site DE-Bay (*Waldstein-Weidenbrunnen*) in the *Fichtelgebirge* mountains (Germany).

We will present an overview of the field experiments within the EGER project, of their design, the applied methods, and particularly of the first results from both Intensive Observation Periods, namely September/October 2007 (IOP-1) and June/July 2008 (IOP-2). Concerning the latter, we focussed our analysis on the coupling between the above-canopy atmosphere and different layers in the canopy due to coherent structures and special atmospheric boundary layer phenomena and its consequences for (i) the structure of the turbulent exchange, (ii) the above-canopy fluxes, (iii) the time scales of turbulent transport and chemical reactions, (iv) the concentration gradients of non-reactive and reactive trace gases between top of the canopy and forest floor, and (v) the consequences for model parameterizations.

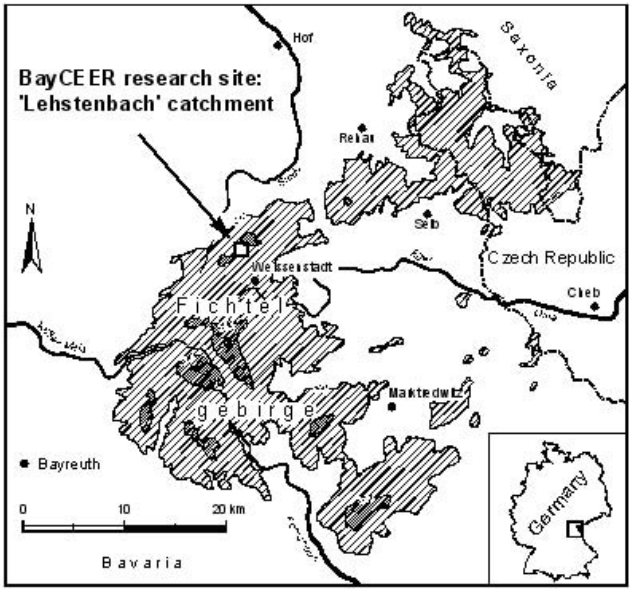

Fig. 1. Map of the "*Fichtelgebirge*" region (Gerstberger et al., 2004). The *Waldstein-Weidenbrunnen* site is located in the *Lehstenbach* catchment north-west of the small town *Weissenstadt* and the upper *Eger river* valley. Hatchings indicates elevations >500 m and >750 m a.s.l, respectively.

2 Material and methods

2.1 Site description

The *Waldstein-Weidenbrunnen* site (50°08′31″ N, 11°52′01″, 775 m a.s.l.) in the *Fichtelgebirge Mountains* (Germany) was selected for the present study. It is located in the *Lehstenbach* catchment in NE Bavaria (Germany), a research area of the Bayreuth Center of Ecology and Environmental Research (BayCEER). The site is also a FLUXNET site (DE-Bay, see Baldocchi et al., 2001) featuring CO_2 flux measurements above the spruce forest since 1996 and intensive ecological and meteorological studies in this area (Matzner, 2004). The site is located NW of the upper *Eger* river valley (Fig. 1). More detailed information of the site can be found in Gerstberger et al. (2004), recently updated by Staudt and Foken (2007) for the EGER project.

The site is dominated by Norway Spruce (*Picea abies*) trees of 25 m canopy height (2008) with a Plant Area Index (PAI) of 5.6 $m^2\,m^{-2}$ for the overstory and of 3.5 $m^2\,m^{-2}$ for the understory (see Appendix A). Based on the PAI profile, the turbulence structure within the *Waldstein-Weidenbrunnen* forest site appears to be similar to those observed at other forest sites: measures of integral turbulence characteristics (σ_u/u_*, σ_v/u_*, σ_w/u_*; where σ_u, σ_v, σ_w: standard deviations of the horizontal (u, v), and vertical (w) wind components; u_*: friction velocity) typically decrease from their values observed in the surface layer (above-canopy = 100 %) to values between 15 and 40 % at 2 m above ground (Amiro,

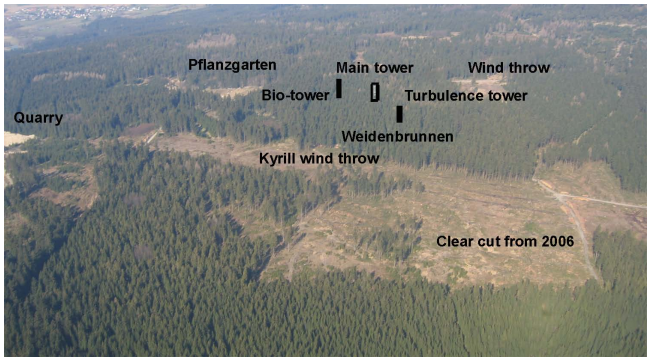

Fig. 2. The *Waldstein-Weidenbrunnen* site shortly after the "hurricane like" low pressure system "Kyrill" (view from south, photograph: T. Foken, 15 March 2007). The "main tower" can be seen within the *Waldstein-Weidenbrunnen* field site; "turbulence" and "bio" towers were set-up after 15 March 2007, but their locations are marked.

1990; Raupach et al., 1996). Inside the forest ($z < h_c$; z: height above ground; h_c: canopy height) the parameterization proposed by Rannik et al. (2003) is closely fulfilled (see Appendix A), and was used in the footprint model for the *Waldstein-Weidenbrunnen* site (Göckede et al., 2006, 2007).

On 18 January 2007, shortly after the start of the EGER project the "hurricane like" low pressure system "Kyrill" destroyed large forested areas south of the *Waldstein-Weidenbrunnen* site (Fig. 2). Results of a footprint analysis performed for the conditions after "Kyrill" (Siebicke, 2008) indicated that "Kyrill" related clear cuts are outside of the major footprint area. It can be assumed that the footprint of the target area "spruce" of *Waldstein-Weidenbrunnen* is not significantly affected by "Kyrill" related wind-throws and clear cuts.

2.2 Intensive Observation Periods (IOPs) of the EGER project

The first Intensive Observation Period (IOP-1) of the EGER project at the *Waldstein-Weidenbrunnen* site took place in September and October 2007, the second in June and July 2008 (IOP-2). Mainly wet autumn weather conditions characterized IOP-1, while sunny summer weather conditions with scattered showers prevailed during IOP-2. An overview of the meteorological conditions and ambient O_3, NO, NO_2, and SO_2 concentrations is given in the Supplement. Wet deposition of the ionic components of rain (in mg m^{-2}), integrated over the entire time period of IOP-1 and IOP-2, are also given in the Supplement and have been found to be typical for the region.

Within the scope of this paper, we have selected for each IOP a so-called "Golden Days" periods to present some of our results: 20 to 24 September 2007 (IOP-1) and 28 June to 2 July 2008 (IOP-2), respectively. As listed in the Supplement (Table S2), these periods were characterized by high radiation, no precipitation and hardly any clouds (to emphasize photochemical aspects of our studies). The "Golden Days" period of IOP-2 was warmer and drier than that of IOP-1, with higher air and soil temperatures, higher maximum water vapour pressure deficits and lower soil moistures. Wind speeds were moderate and comparable for both "Golden Days" periods.

2.3 Measurements

2.3.1 General set-up of towers and instrumentation

The so-called "main tower" (31 m, walk-up type) of the *Waldstein-Weidenbrunnen* site (see Fig. 2, Fig. S1 of Supplement) served for standard meteorological measurements (e.g. vertical profiles of wind velocity, dry and wet bulb temperature) as well as for the measurements of vertical profiles of trace gas concentrations and trace gas fluxes. An additional, 35 m tall and slim tower for turbulence measurements was set up approx. 60 m south-east of the "main tower". 60 m north-west of the "main tower" another walk-up tower ("bio-tower") for plant physiological measurements was installed (see Fig. 2, Fig. S1 of Supplement).

In complex terrain like the *Waldstein-Weidenbrunnen* site, monitoring of the atmospheric boundary layer's structure became an important tool for interpretation of the turbulent exchange data. For corresponding monitoring a composite of several remote sensing instruments was used: the sodar/RASS (METEK GmbH) and the mini-sodar (Scintec AG) system at the *Waldstein-Weidenbrunnen* site, and the 482 MHz-windprofiler (Vaisala) of the German Meteorological Service about 25 km south of the field site. For more details see Supplement and Serafimovich et al. (2008a, b).

2.3.2 Measurements of turbulent fluxes

As shown in Table 1, six levels of the "turbulence tower" and up to four levels of the "main tower" have been equipped with 3-D sonic anemometers, most of them also with fast-response open-path CO_2 and H_2O analyzers, some of them with fast-response O_3 analyzers, and one level in IOP-2 with the intake for fast-response measurements of NO and NO_2 concentrations. The EUROFLUX methodology (Aubinet et al., 2000) and recent updates of the TK2 software (Mauder and Foken, 2004, 2011; Mauder et al., 2008) provided the basis of all calculations for the turbulent fluxes of momentum, sensible heat, latent heat, CO_2, O_3, NO, and NO_2. Furthermore, all flux measurements for the *Waldstein-Weidenbrunnen* site were footprint controlled (Foken and Leclerc, 2004; Göckede et al., 2004, 2006) and data quality checked (Foken and Wichura, 1996; Foken et al., 2004). The coordinate system for all 3-D wind measurements was chosen parallel to the stream lines using the planar-fit method (Wilczak et al., 2001).

Table 1. Turbulent flux measuring instrumentation at the *Waldstein-Weidenbrunnen* site during the Intensive Observation Periods of the EGER project (IOP-1: 2007; IOP-2: 2008).

	Height [m]	Sonic anemometer	Trace gas	Trace gas analyzer
"main tower" (IOP-1)	32	Solent R2, Gill Instruments Ltd.	CO_2, H_2O	LI-7500, L-COR Inc.
			O_3	GEFAS GmbH[3]
	1[4]	Solent R2, Gill Instruments Ltd.	O_3	GEFAS GmbH[3]
"main tower" (IOP-2)	32	USA-1, METEK GmbH	CO_2, H_2O	LI-7500, L-COR Inc.
	32	CSAT3, Campbell Sci. Inc.	NO, NO_2	CLD 790SR-2, Ecophysics
			O_3	NOAA/ATDD[3]
	25	Solent R2, Gill Instruments Ltd.	O_3	Enviscope GmbH[3]
	17	Solent R2, Gill Instruments Ltd.	O_3	Enviscope GmbH[3]
	1	Solent R2, Gill Instruments Ltd.	O_3	GEFAS GmbH[3]
"turbulence tower" (IOP-1, IOP-2)	36	USA-1, METEK GmbH	CO_2, H_2O	LI-7500, L-COR Inc.
	23	CSAT3, Campbell Sci. Inc.	CO_2, H_2O	LI-7500, L-COR Inc.
	18	Solent R3-50, Gill Instrum. Ltd.	CO_2, H_2O	LI-7500, L-COR Inc.
	13	CSAT3, Campbell Sci. Inc.	CO_2, H_2O	LI-7500, L-COR Inc.[2]
	5.5	CSAT3, Campbell Sci. Inc.[1]	CO_2, H_2O	LI-7500, L-COR Inc.
	2.5	CSAT3, Campbell Sci. Inc.	CO_2, H_2O	LI-7500, L-COR Inc.

[1] During IOP-1 Solent R2, Gill Instruments Ltd.
[2] During IOP-1 KH20 Campbell Scientific, Inc.
[3] All fast-response O_3-analyzers were based on solid-phase chemiluminescence technique (Güsten and Heinrich, 1996), but designed by different manufacturers (indicated)
[4] O_3-flux measurements at 1 m have been performed one week before those at 32 m (using the same instrumentation)

During IOP-1, only turbulent O_3 fluxes, during IOP-2 also turbulent fluxes of NO and NO_2 were measured using eddy-covariance systems. In case of NO and NO_2, high frequency (5 Hz) time series of NO and NO_2 concentrations were recorded with a specialized, fast-response, state-of-the-art, high precision 2-channel NO-NO_2 chemiluminescence analyzer (model CLD 790SR-2, Ecophysics, Switzerland). While one channel was used for the direct measurement of the NO concentration, the measurement of the NO_2 concentration was indirect, following high efficiency conversion of NO_2 to NO (through two up-stream solid state blue light converters in series) and consecutive NO detection in the second channel of the chemiluminescence analyzer. To maintain continuous time series of the fast-response NO and NO_2 measurements, NO and NO_2 signals have not been calibrated on-line; instead, they have been related to NO and NO_2 concentrations which were measured side-by-side by slow-response NO-NO_2 chemiluminescence analyzers (see Sect. 2.3.3). The analyzers revealed detection limits (3σ-definition) ranging between 0.05–0.12 ppb (NO) and 0.22–0.76 ppb (NO_2), respectively; data found to be below the limit of detection have been discarded. A 53 m long insulated bundle containing the Teflon® inlet tubes, tube heating as well as interface cables from the data logger ran from the top of the "main tower" to the analyzer and control computers in a nearby air-conditioned shelter (container). In the case of O_3, high frequency (20 Hz) time series of O_3 concentration were recorded by fast-response solid-phase chemiluminescence analyzers (Güsten and Heinrich, 1996) designed by different manufacturers (see Table 1). Solid-phase chemiluminescence analyzers provide O_3 concentration only in relative units (voltage), and the analyzers' sensitivity is not temporally constant (due to the influence of relative humidity on the chemiluminescent dye). However, absolute O_3 concentrations were simultaneously measured side-by-side each fast-response O_3-analyzer by slow response UV-absorption based ozone analyzers (see Sect. 2.3.3). Based on these data, fast-response O_3 signals could be converted to O_3 concentrations and hence, after applying the above mentioned procedures for correction and quality check of eddy-covariance measurements, the turbulent O_3-fluxes and deposition velocities were calculated.

2.3.3 Profile measurements

Measurements of the vertical profiles of wind speed and dry and wet bulb temperatures are part of a standard and continuously running monitoring programme at the *Waldstein-Weidenbrunnen* site (www.bayceer.de). Cup anemometers, characterized by low distance constant (approx. 3 m), and Frankenberger type psychrometer (Frankenberger, 1951), all equipped with high precision sensors, have been mounted at different levels along the "main tower" (see Table 2). During both IOPs, these sensors have been amended by additional wind speed sensors (A100ML, Vector Instr., UK) and home-built, thermocouple-based psychrometers (see Table 2).

Along the "main tower", vertical profiles of CO_2, H_2O, NO, NO_2, and O_3 concentrations were measured at nine

Table 2. Profile measurements at the "main tower" of the *Waldstein-Weidenbrunnen* site during the Intensive Observation Periods of the EGER project (IOP-1 and IOP-2).

	IOP-1 6 September–7 October 2007	IOP-2 1 June–15 July 2008
	measurement levels at "main tower" (in m)	
wind speed I wind speed II	4.6, 10.0, 16.5, 18.0, 21.0, 25.0, 31.0 4.6, 10.0, 16.5, 18.0, 21.0, 25.0, 31.0	7.6, 13.3, 19.8, 24.3, 26.3, 31.3 7.6, 13.3, 19.8, 24.3, 26.3, 31.3
dry and wet bulb temperature I (aspirated) dry and wet bulb temperature II (aspirated)	5.0, 13.0, 21.0, 31.0 4.9, 9.9, 15.9, 19.5, 24.4, 26.6, 30.9	5.0, 13.0, 21.0, 31.0 4.9, 9.9, 15.9, 19.5, 24.4, 26.6, 30.9
CO_2, H_2O, O_3, NO, NO_2	5.0, 10.0, 16.0, 24.2 (2×), 31.0	3.0, 10.0, 16.5 (2×), 20.5, 25.0, 31.5
NH_4NO_3, NH_3 and HNO_3	24.2, 30.4	N/A
HONO	24.5	N/A
NO, NO_2, O_3, CO_2 and H_2O exchange measurements on spruce branches (dynamic cuvette)	13.0	N/A
	measurement levels at "forest floor" (in m)	
wind speed I wind speed II	2.0 0.04, 0.30, 1.0, 2.00	2.0 0.04, 0.3, 1.0, 2.0
dry and wet bulb temperature I (aspirated) dry and wet bulb temperature II (aspirated) air temperature (non-aspirated)	0.05, 2.0 0.09, 0.26, 1.00, 2.05 0.01, 0.02, 0.04, 0.08, 0.16, 0.32	0.05, 2.0 0.09, 0.26, 1.00, 2.05 0.01, 0.02, 0.04, 0.08, 0.16, 0.32
CO_2, H_2O, O_3, NO, NO_2	0.05, 0.3, 1.0, 2.0	0.005, 0.03, 0.1, 0.3, 0.9
$^{220}Rn/^{222}Rn$	0.04, 0.27	0.00, 0.03, 0.1, 0.3
HONO	0.5	1.0
	measurement levels at "bio-tower" (in m)	
air temperature and rel. humidity (aspirated)	9.3, 11.7, 14.8, 17.2, 20.2, 22.6	9.3, 11.7, 14.8, 17.2, 20.2, 22.6
net radiation	11.9, 17.4, 22.8	11.9, 17.4, 22.8
CO_2	N/A	0.03, 1.0, 16.0, 18.7, 21.4, 24.1, 29±3, 36.0

(IOP-1) and eleven (IOP-2) levels, respectively (see Table 2). Due to the limited absolute accuracy (but generally much better precision) of the trace gas analyzers, concentrations from different levels have been measured sequentially by one set of analyzers in order to resolve even small vertical differences of concentrations. To keep the time period required to "scan" the full profile short (<30 min), two identical but independently operating sets of analyzers have been deployed. One set was applied to levels of the upper part of the profile (>24 m, IOP-1; >16.5 m, IOP-2), the other set for the lower levels of the profile (i.e. within canopy and particularly close to the soil-trunk space interface). Both sets of analyzers had overlapping levels (24 m, IOP-1; 16.5 m, IOP-2), where concentration measurements (from side-by-side intakes) provided a continuous data set to cross-check (and to correct) for systematic offsets. Ambient air was drawn from the different intake levels through heated and insulated PTFE-tubing (4.1 mm inner diameter; opaque; length: 55 m each) into an air-conditioned container (housing the two sets of analyzers) on the forest floor close to the "main tower". All sampling lines were continuously purged, and the "active" sampling line was sequentially switched between the

different levels (switching interval: 1.5 min). NO and NO_2 concentrations were measured by 1-channel chemiluminescence analyzers (CLD TR-780, Ecophysics, Switzerland). NO was detected first, then NO_2, after the sampling air has passed a solid-state blue light converter (installed upstream from the analyzer for species specific conversion of NO_2 to NO). Detection limits (3σ) for NO and NO_2 during the experiments were <0.12 and <0.76 ppb, respectively. Precision was <0.6 % (10 ppb NO) and <4 % (20 ppb NO_2), respectively. For measurements of O_3 concentrations, UV absorption spectrometers (TEI 49c/I, Thermo Electron, USA) which had a precision <2 % were used. Concentrations of CO_2 and water vapour were measured by NDIR absorption analyzers (Li-7000 and Li-840, LI-COR Biosiences, USA); corresponding precision was <0.2 % for both CO_2 and H_2O. All analyzers were calibrated at least weekly, using certified CO_2 standards (pressurized cylinders), a dew point generator (Li-COR Biosiences, USA), and a certified NO standard (5 ± 0.09 ppm, Air Liquide, Germany) in combination with a gas-phase-titration unit (model 146c, Thermo Electron, USA) to generate suitable concentrations of NO, NO_2, and O_3.

During IOP-1, concentrations of the NH_3-HNO_3-NH_4NO_3 triad were measured at two heights above the forest canopy using a novel wet chemical instrument, the GRAEGOR (GRadient of AErosols and Gases Online Registrator, Thomas et al., 2009). Gaseous NH_3 and HNO_3 and particulate NH_4NO_3 constitute a thermodynamic equilibrium which strongly depends on relative humidity and temperature as well as on aerosol composition, especially SO_4^{2-} concentrations (Mozurkewich, 1993; Nenes et al., 1998; Stelson and Seinfeld, 1982). GRAEGOR is capable of measuring the interacting species gaseous NH_3 and HNO_3 as well as particulate NH_4^+, NO_3^-, and SO_4^{2-} selectively and simultaneously at two different heights. For the first time, such highly time resolved measurements of the complete triad were performed above a forest canopy. The instrument was thoroughly characterised for its ability to resolve vertical concentration differences above the forest (and a grassland site) for a range of atmospheric conditions (Wolff et al., 2010). From the experimentally determined errors of the concentration differences the resulting flux errors were estimated. For the *Waldstein-Weidenbrunnen* forest experiment median instrumental flux errors were: 50 % (NH_3), 38 % (HNO_3), 57 % (NH_4^+), and 68 % (NO_3^-), respectively (Wolff et al., 2010).

During both IOPs, ambient HONO mixing ratio were measured with a wet-chemical instrument, the Long Path Absorption Photometer (LOPAP, Kleffmann et al., 2002; Heland et al., 2001). This underlying technique offers a high temporal resolution (5–7 min) and a very low detection limit of about 0.001 ppb. During IOP-1, we had set up two LOPAP instruments, one close to the forest floor (0.5 m) and the other one just above the canopy (24.5 m). The data set provides valuable information to study potential HONO formation processes on the different surfaces, which may be heterogeneous or even photo-enhanced sources of HONO.

2.4 Analysis of coupling

As stated in the introduction, the experimental and also the modelling design of this study was based on the analysis of the spatial and temporal scales of the relevant exchange processes in the forest, atmosphere, plants and soil. The application of the scheme given in Appendix B needs further improvements when the coupling between the above-canopy atmosphere and the canopy was taken into account. Here, turbulent time scales must be compared not only with characteristic time scales of chemical reactions, which is forms the Damköhler number – see Supplement for calculation according to Mayer et al. (2011) and Lenschow (1982) – but also with the time scales of coherent structures.

Coupling between the above-canopy atmosphere and the canopy is related to the development of the mixing layer, which for the *Waldstein-Weidenbrunnen* site has already been studied in detail (Thomas and Foken, 2007a; Wichura, 2009; Wichura et al., 2004). For the *Waldstein-Weidenbrunnen* site the characteristic length scale of the mixing layer

$$L_s = \delta_w / 2 = \frac{u(z_B)}{\left(\partial u / \partial z\right)_{z=z_B}} \quad (1)$$

was found to be on the order of 7–8 m in day time and 6–7 m in night time except in the SE sector where it was only 5 m. Therefore, with the wavelength of the initial Kelvin-Helmholtz instability Λ_x a linear relation exists between both scales (Raupach et al., 1996)

$$\Lambda_x = m\, L_s, \quad (2)$$

The coefficient m ranged from 7–10 and for the SE sector up to 16 (Thomas and Foken, 2007a). This was found in 2003 for a canopy height of about 19 m. Following the determination of the thickness of the roughness sublayer (z_*) according to Verhoef et al. (1997) namely $z_* = h_c + cL_s$ with $c = 2...3$, it follows for the *Waldstein-Weidenbrunnen* site that z_* was approx. 40 m (2003), for the present canopy height about 50 m, and in the SE sector even less. This is much lower than for other sites (Mölder et al., 1999), probably because of the special location of the *Waldstein-Weidenbrunnen* site near a ridge.

The wavelength of the initial Kelvin-Helmholtz instability is also necessary to determine the flux contributed by coherent structures between different layers in the canopy and the above-canopy atmosphere (Thomas and Foken, 2007b). Thereby the coherent structures were detected with a wavelet tool (Thomas and Foken, 2005). Using turbulence measurements in three levels (above canopy, top of the canopy, and trunk space) the coupling between these levels by coherent structures can be exactly detected. This is for tall vegetation

a tool which covers also complicated night time situations with sudden coupling/decoupling events. Due to counter gradients these nighttime events are not detected with the coupling analysis based on stratification only as used by Steiner et al. (2011). For most other cases both methods give equal results. On this basis an exchange classification was proposed, and a brief description is given for the five coupling regimes:

Wave motion (Wa). The flow above the canopy is dominated by linear wave motion rather than by turbulence (Thomas and Foken, 2007a; Cava et al., 2004).

Decoupled canopy (Dc). The air above the canopy is decoupled from the canopy and subcanopy.

Decoupled subcanopy (Ds). The atmosphere is coupled with the canopy, but decoupled from the subcanopy. The region of coherent exchange is limited to the canopy.

Coupled subcanopy by sweeps (Cs). The exchange between the above-canopy air and the subcanopy is forced by the strong sweep motion of coherent structures only.

Fully coupled canopy (C). The atmosphere, the canopy and the subcanopy are in a fully coupled state.

2.5 Modelling

The ACASA model (Advanced Canopy-Atmosphere-Soil Algorithm, Pyles, 2000; Pyles et al., 2000) is a multi-layer model that incorporates a third-order closure method to calculate turbulent transfer within and above the canopy (Meyers, 1985; Meyers and Paw U, 1986, 1987). Such a higher order closure method overcomes the limitations of turbulence modules found within many stand-scale models that apply the flux-gradient relationships (K-theory) within forest canopies (Denmead and Bradley, 1985; Shaw, 1977). Important features of the ACASA model are: long- and shortwave radiative transfer within the canopy (Meyers, 1985), the calculation of leaf, stem and soil surface temperatures using the fourth-order polynomial of Paw U and Gao (1988); plant physiological response to ambient conditions by the use of a combination of the Ball-Berry stomatal conductance (Leuning, 1990; Collatz et al., 1991) and the Farquhar and von Caemmerer (1982) photosynthesis equation following Su et al. (1996) and a soil module adapted from MAPS (Mesoscale Analysis and Prediction System, Smirnova et al., 1997, 2000).

The model STANDFLUX (Falge et al., 1997, 2000) provides a framework for integrating three-dimensional aspects of forest stand structure and light interception, one-dimensional vertical aspects of stand microclimate, and gas exchange behaviour of plant organs distributed throughout a forest stand. It consists of three nested components with a leaf or branch gas exchange module at the innermost level (for needled portions of branches), a three-dimensional single-tree light interception and gas exchange module as the next step in the hierarchy, and a three-dimensional forest-stand gas exchange model occupying the outermost shell. The model structure is designed for separate validation at each organizational level. Predicted net photosynthesis and conductance of foliage elements (for spruce needled branch ends) can be compared with dynamic cuvette gas exchange measurements and simulated single tree transpiration results with xylem sap flow estimates, while stand level predictions may be validated via eddy-covariance measurements.

Results from measurements of a portable gas exchange system (GFS3000, Walz, Effeltrich, Germany) enabled us to parameterize the response of needle CO_2 and H_2O exchange under assorted micrometeorological factors during the field campaigns. Parameters for a leaf gas exchange model (Farquhar type) were derived, utilizing information from both single factor dependencies on light, temperature, CO_2 concentration, and relative humidity, and diurnal time course measurements of gas exchange.

3 Results and discussion

The following sections concentrate on two fair weather periods in both IOPs, namely 20–24 September 2007 (fall, DOY 263–267, IOP-1), and 29 June–2 July 2008 (summer, DOY 181–184, IOP-2). Both periods were characterized by high and nearly identical radiation fluxes, no precipitation, hardly any clouds and very similar wind forcing. This facilitates the comprehensive interpretation of our first results, particularly with respect to photochemical aspects.

3.1 Coherent structures – coupling between the atmosphere and canopy

The method described in Sect. 2.4 gives us the opportunity not only for the determination of coupling stages but also to separate the flux into a Reynolds averaged flux and a flux transported by coherent structures (upper panel in Fig. 3). The Reynolds-averaged flux is derived using the triple decomposition of the instantaneous turbulent flow variable (Bergström and Högström, 1989). To estimate the contribution of coherent structures to the fluctuation conditional sampling analysis and averaging over the time period of their occurrence were applied (Antonia, 1981). Moreover, applying the averaging operator within the occurrence of sweep or ejection motions, contributions of ejection and sweep events to the individual fluxes are determined, respectively (Collineau and Brunet, 1993b).

In general the contribution of coherent structures to the total flux is 20–30 %, sometimes lower at daytime and in the late evening, during night often higher than 50 %. Furthermore, it was found that momentum and sensible heat transport by coherent structures is dominant in the canopy and

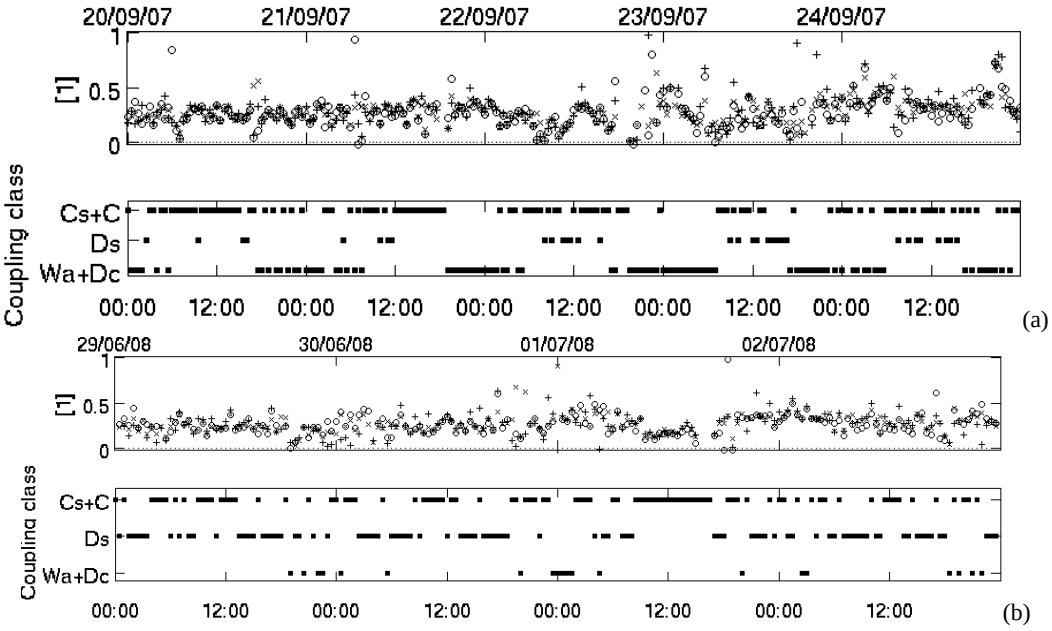

Fig. 3. Measurements and characterisation of the turbulent exchange for the period 20 to 24 September 2007 during IOP-1 **(a)** and 29 June to 2 July 2008 during IOP-2 **(b)**. Upper panel: relative flux contribution of coherent structures $F_{cs}F_{tot}^{-1}$ for carbon dioxide (open circles), buoyancy (crosses) and latent heat (pluses) flux at $1.44\,h_c$; lowest panel: coupling situations.

CO_2 and H_2O transport by coherent structures increases with height within the canopy and reaches a maximum at the upper canopy level. The flux contribution of the ejection and sweep phase of coherent exchange were also determined. The flux contribution of the ejection phase decreases with increasing height within the canopy and becomes dominant above the canopy level. The flux fraction transported during the downward directed sweep phase increases with height within the canopy and becomes the dominating exchange process at the upper canopy level. Within the sub-canopy space, close to the ground surface, ejection and sweep phases contribute equally to the individual fluxes. This issue is discussed in more detail by Serafimovich et al. (2011). The coupling classification for both IOPs is shown in Fig. 3.

Conditional sampling analysis demonstrates domination of coherent structure signatures in vertical wind measurements (Serafimovich et al., 2011) with potential time scales in the range 10 to 40 s. The number of coherent structures detected at the turbulence tower is lowest directly under the crown (5 m above ground) and higher in the trunk space and above the canopy with a maximum at the canopy level. Most of the structures were found for vertical wind velocity, followed for air temperature. There were more structures found in H_2O flux than in the CO_2 flux.

Coupling classification was used in the following sections for a better understanding of the behaviour of trace gas concentrations. First analysis showed that the attribution of coupling states into classes C and Cs as well as W and Dc is difficult. Therefore, coupling classes C/Cs and W/Dc were combined to obtain a more significant picture of the results. Statistics of coupling classes are shown in Fig. 4 for both IOPs.

The striking difference between IOP 1 and 2 is the dominance of class W/Dc in the autumn (IOP-1), whereas in the summer (IOP 2) the case Ds is dominating comparing the same time periods. But cases of well coupled situations are not significantly different for both IOPs. Typical asymmetry in the stability, namely stronger unstable situations in the morning, already stable situations in the afternoon, and strongest stable situation in the first half of the night can easily be seen in the distribution of the coupling classes as well (see Fig. 3). Obviously, IOP 2 resembles the oasis effect (necessary energy of evaporation is on the cost of sensible heat flux, see Stull, 1988) showing stronger decoupling already in the hours 15–18 which is usually not expected before the hours 18–21 (e.g. IOP-1). Good coupling was found in the nights of both IOPs, probably connected with low-level jets and gravity waves (see Sect. 3.2).

3.2 Influence of the atmospheric boundary layer

To understand the influence of the atmospheric boundary layer's dynamics on surface exchange processes, information about the spatio-temporal behaviour of the boundary layer's temperature and wind fields must be known. Measurements of the two sodar systems showed good agreement at those height intervals, which are covered by both systems. Also, upper levels of sodar and windprofiler measurements showed only very small differences. Therefore, the results of the

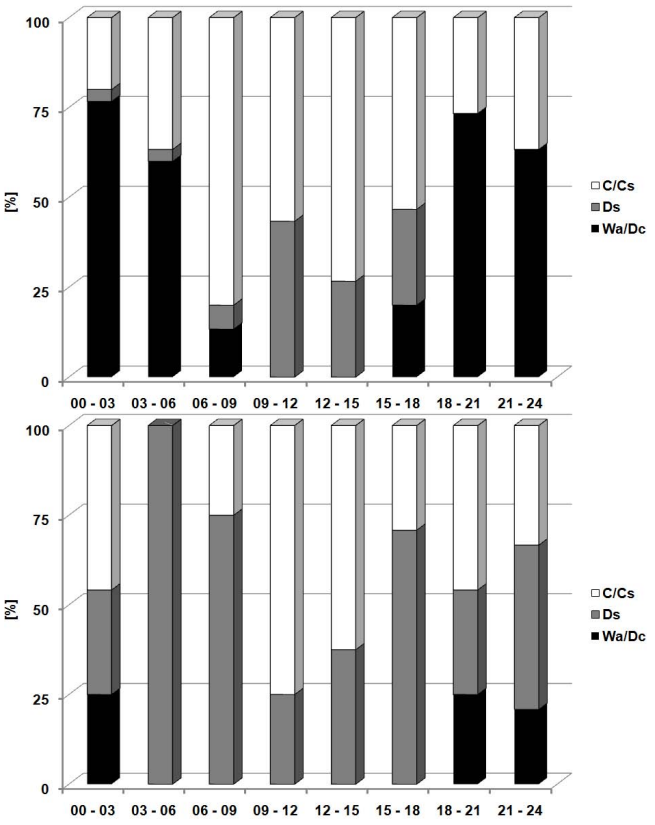

Fig. 4. Percentage of different coupling classes during the Golden Days of IOP-1 (left, 30 three-hour periods) and IOP-2 (right, 24 three-hour periods) in the daily cycle.

three systems were combined to make available a composite picture of the boundary layer structure.

Low-level jets (LLJ), already found in 2003 (Thomas et al., 2006), were investigated more carefully and found to be similar to those in other studies (Banta et al., 2002). Such LLJs were selected, where the wind velocity above and below the jet was at least $2\,m\,s^{-1}$ lower (Stull, 1988) and the duration of LLJs was longer than 90 min. An example is shown in Fig. 5. The wind velocity of the jet was found to be above $10\,m\,s^{-1}$ for about 6 h at a height of 300 m, temporally decreasing down to 200 m. The wind direction of the LLJ was SE, while above the LLJ the wind direction moved from SE over S to W. In the LLJ the vertical wind was negative (downward). During IOP-1 LLJs were found on nine nights, mainly at about 150 m (above ground) with a typical wind velocity of $9\,m\,s^{-1}$. During the summer IOP-2 LLJs were found on 11 nights but typically at 250 m height with about $10\,m\,s^{-1}$.

Turbulent CO_2 fluxes at 32 m (above ground) are also shown in Fig. 5. Generally, very small CO_2 fluxes (during calm periods) following early evening hours have been observed and large CO_2 fluxes during LLJ periods. Karipot et al. (2006, 2008) observed enhanced CO_2 fluxes up to 9–15 $\mu mol\,m^{-2}\,s^{-1}$, though u_* values increased only just above $0.2\,m\,s^{-1}$. This is an indication that during intermittent turbulent periods associated with features such as sporadic jets, high CO_2 fluxes are possible from the large fluctuations in the surface layer accumulated CO_2, in phase with moderate vertical velocity fluctuations. CO_2-rich ejections from the canopy contribute more to the positive (upward) total flux during weak-LLJ events. For the LLJ shown in Fig. 5 similar conditions were found during IOP-2 with an increase of the friction velocity and of the CO_2 flux from 4 to 8 $\mu mol\,m^{-2}\,s^{-1}$.

In Fig. 6, vertical distributions of NO, NO_2, O_3 and CO_2 concentrations are shown during the LLJ event shown in Fig. 5. Due to the increased shear a better mixing was found during the period with the LLJ between 02:00 and 08:00, with a maximum at 04:00. The better mixing resulted – for all trace gases – in a reduction of concentrations accumulated near the surface (Fig. 6). In the early morning, at approximately 04:00, when the LLJ occupied lower heights, the atmosphere close to the surface is suddenly mixed resulting in high NO_2 concentrations, probably an outflow of the upper Eger river valley during easterly winds. However, this picture contains some other features. The most impressive is the inflow of fresh air with low NO_2 and high O_3 concentrations between 22:00 and 24:00, connected with the occurrence of gravity waves. For high NO (and NO_2) concentrations during the morning hours (06:00–12:00), see Sect. 3.3.

3.3 Influence of advection

Although advection is very important for the trace gas balance of a forest (Finnigan, 2008), the substantial problem, posed by the ability to measure the advection, has still not been solved. The classical approach addressing a more or less steady-state flow through a volume element was, in many experiments, unsuccessful (Aubinet et al., 2010; Aubinet, 2008; Feigenwinter et al., 2008). Nevertheless, this approach was also tested on the *Waldstein-Weidenbrunnen* site in 2003 and during both IOPs. Even very careful analysis of the data, including a planar fit analysis (Wilczak et al., 2001) adapted to the process, could not provide the necessary progress (Siebicke et al., 2011a). Therefore, Siebicke (2011) applied the coupling concept to the study of advection and tried to explain the measured horizontal CO_2 gradients with the complex structure of the canopy and understory of the *Waldstein-Weidenbrunnen* site. He found significant correlations between the horizontal gradients, which were determined on the basis of high time resolution CO_2 concentration measurements during IOP-2 (Siebicke et al., 2011b), and the duration and intensity of coherent structures.

Concerning the interpretation of fluxes and vertical concentration gradients of the NO-NO_2-O_3 triad, the *Waldstein-Weidenbrunnen* site shares a rather general problem with any other site located in polluted, but also in rural areas (e.g. Alaghmand et al., 2011): the proximity to

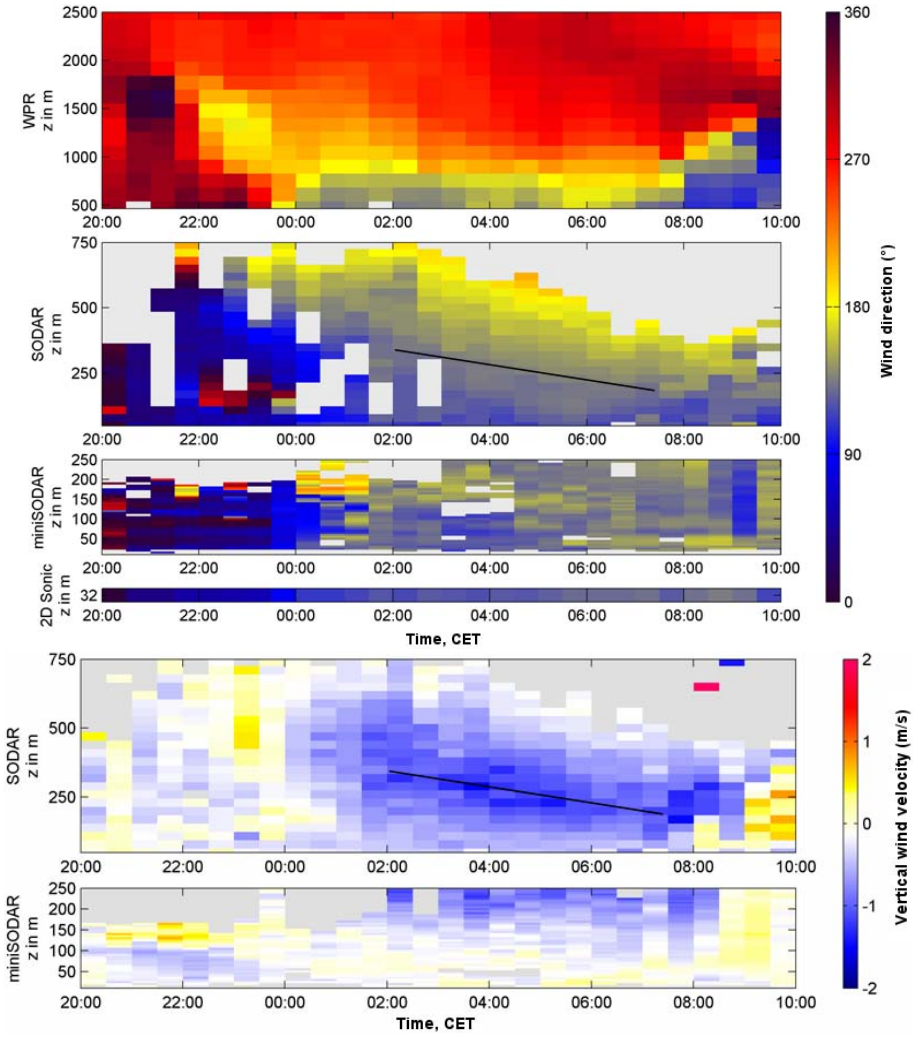

Fig. 5. Time-high profile from windprofiler, sodar, mini-sodar and sonic data of the wind direction (above), and vertical wind velocity (below) in the night from 30 June to 1 July 2008. The axis of the low-level jet is highlighted.

anthropogenic sources of NO_x (industrial, domestic and/or traffic). Within the dispersion plume close to these sources, freshly emitted NO of high concentration (several hundreds of ppb) titrates ambient O_3 and starts the formation of NO_2. However, it depends upon the day/night situation, on the actual boundary layer stability regime, and above all on the distance of the site to the source, to what extent flux and concentration gradient measurements will be biased by advection of high NO (or NO_2) concentrations. In the case of the *Waldstein-Weidenbrunnen* site, the unavoidable NO source consists of the nearby district road (HO18), characterized by a rather high traffic volume of 2100 cars per day (working days). The nearest distance of HO18 to the site is about 1.2 km. However, since main wind sectors of the site are SW to NW, and HO18 runs west of the site from SSE to NNW, "advective disturbance" of desired homogeneous concentration fields is more than likely. Exemplarily for the entire periods of IOP-1 and IOP-2, NO concentrations, measured with 5 Hz resolution (see Sect. 2.3.2) above the canopy (32 m above ground), have been averaged to 30 min means and are shown for the "Golden Days" period of IOP-2 in Fig. 7. NO concentrations are observed every day to increase strongly at 06:00, reaching maximum values around 09:00, and to decline to <0.1 ppb after noontime. The early morning increase can definitely be attributed to the emission and subsequent accumulation of NO in the still existing shallow nocturnal boundary layer over the site with the begin of the commuting traffic (to district capitals Hof and Bayreuth) which starts at 05:30–06:00. Until 09:00, high NO concentrations (30 min averages) are associated with large standard deviations, indicating high variability and consequently low stationarity of NO concentrations. Noticeable growth of the daytime convective boundary layer (after 10:00) leads to substantial dilution of traffic emissions and consequently to much lower NO concentrations at the site.

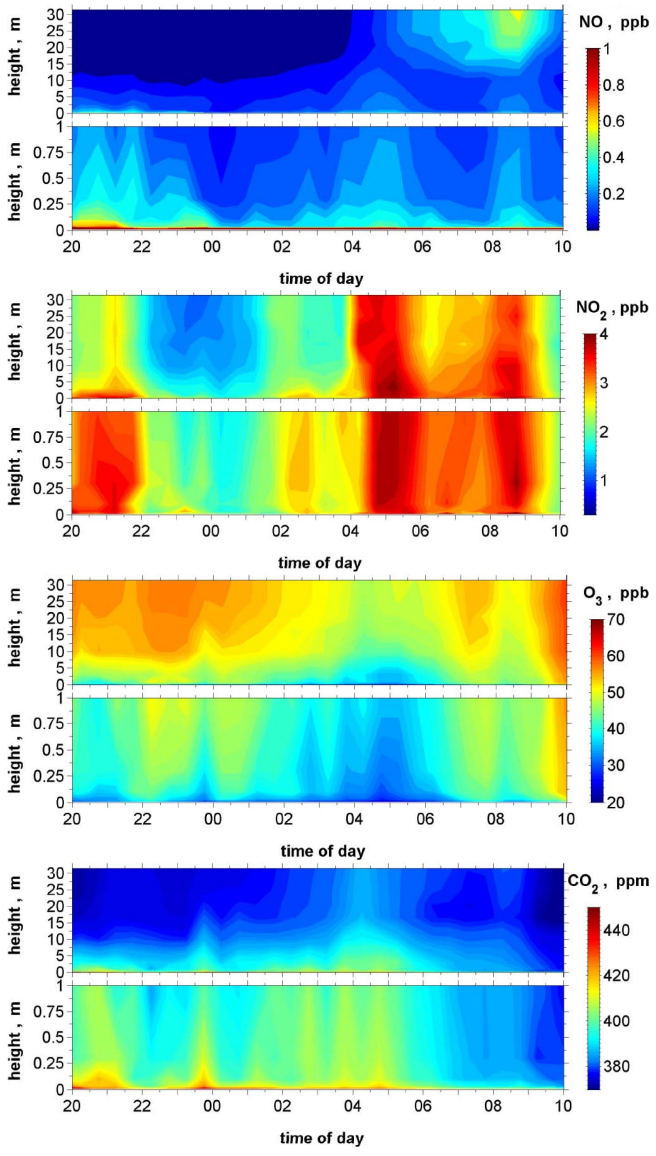

Fig. 6. Averaged vertical profiles in the night from 30 June to 1 July 2008 (compare with Fig. 5) for NO, NO_2, O_3 and CO_2 time in CET.

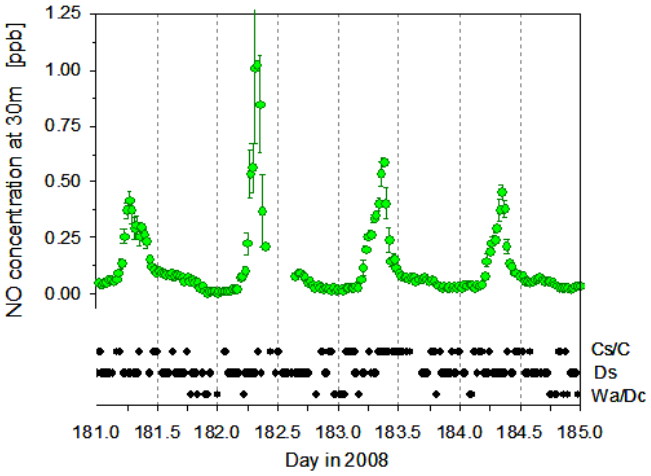

Fig. 7. Diel variation of NO concentration measured at *Waldstein-Weidenbrunnen* main tower (above canopy; 30 m above ground) from 29 June to 2 July 2008 (IOP-2). Every day, between 06:00 and 12:00 (CET), when the convective boundary layer was still emerging, particularly high NO concentrations with large standard deviations were observed due to advection of freshly emitted exhaust gases from a busy (2100 cars/day) district road (HO18) running from SSE to NNW between 1 and 2 km distance west to the *Waldstein-Weidenbrunnen* site. The occurrence of canopy coupling stages (Cs/C, Ds, Wa/Dc) is given at the bottom.

When enhanced NO concentrations from the district road arrive at any position of the forest edge, the actual surface layer flow will transport the NO from there to the measurement site. This will lead, particularly for NO, to the generation of chemically induced vertical concentration gradients: the wind speed at the forest floor is approximately one order of magnitude lower than above the canopy. This, in turn, allows a tenfold longer time for O_3 to react with NO at the forest floor. The reaction product NO_2, however, will be photolyzed back to NO above the canopy, while in the shadow at the forest floor this reaction is at least strongly suppressed. Both effects lead at the measurement site, finally, to noticeable differences of NO concentrations between above canopy and forest floor. A clear example is shown in the upper panel of Fig. 6, where a vertical NO gradient (between 31.5 m and 0.9 m above ground) of $\geq$0.3 ppb was observed during 08:00–10:00 (1 July 2008).

Since in the presence of strong horizontal advection and low stationarity of concentrations the interpretation of measured fluxes and/or vertical gradients in terms of turbulent exchange is generally not meaningful, we omitted all NO, NO_2, and O_3 data measured between 06:00 and 12:00 CET from our analysis in Sects. 3.4. and 3.5.

3.4 Trace gas fluxes

All turbulent fluxes, measured at 32 m above ground (as well as time scales, Damköhler numbers, and concentration differences, Sect. 3.5), have been classified two-fold, (a) by day- and night-time (defined by time of sunrise and sunset, and (b) by corresponding coupling regimes Dc/Wa, Ds, Cs/C, and then summarized into box-and-whisker plots. Figure 8 shows the results of classification (according to Wa/Dc, Ds, Cs/C coupling stages) of turbulent fluxes of water vapor (F_{H_2O}), carbon dioxide (F_{CO_2}), ozone (F_{O_3}), nitrogen dioxide (F_{NO_2}), nitric oxide (F_{NO}), total ammonium ($F_{NH_4^+,tot}$), and total nitrate ($F_{NO_3^-,tot}$). It has to be kept in mind that daytime temperature of the air (T_{air}) and relative humidity (RH) showed relatively similar medians and dispersion for the three different coupling regimes. In contrast, daytime median and variation of global radiation data (Rg) were much lower during the coupling regime Wa/Dc as compared

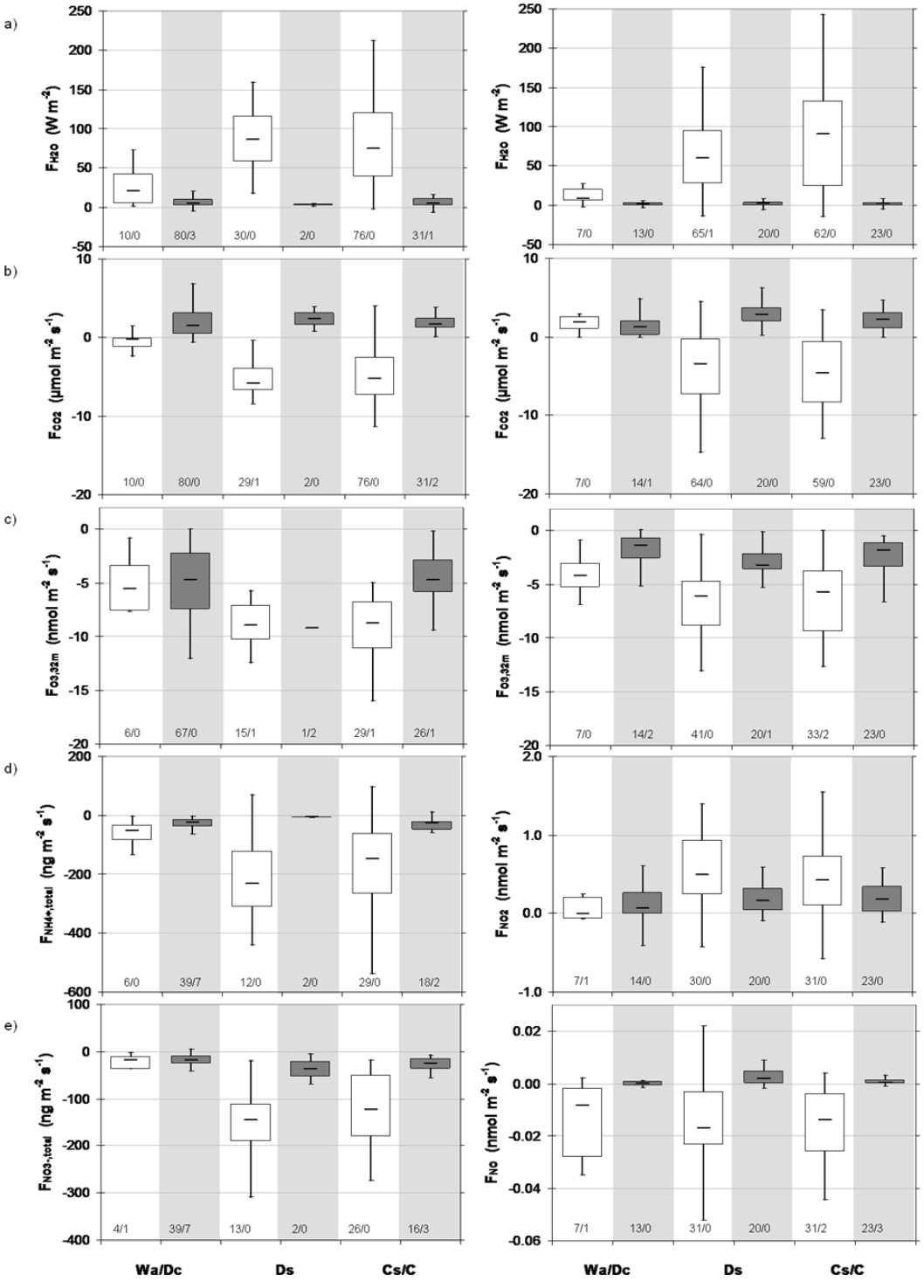

Fig. 8. Statistical dispersion and skewness of turbulent fluxes (F) of gaseous and particulate trace compounds at the "main tower" for 20–24 September 2007 (IOP-1, DOY 263-267, left panels) and for 29 June to 2 July 2008 (IOP-2, DOY 181–184, right panels): F_{H_2O} **(a)**, F_{CO_2} **(b)**, F_{O_3} **(c)**, $F_{NH_4^+,tot}$ (**d**, left panel), F_{NO_2} (**d**, right panel), $F_{NO_3^-,tot}$ (**e** left panel), and F_{NO} (**e** right panel). Data were classified by coupling regimes (Wa/Dc, decoupled conditions; Ds, decoupled subcanopy; Cs/C, coupled subcanopy by sweeps and fully coupled subcanopy) and day- (open box-plots) and night-time (grey shades). Remark: the bottom and top of each box represent the 25th and 75th percentile, the horizontal bar within each box is the 50th percentile (median); horizontal bars at the end of the whiskers stand for the lowest (highest) value still within 1.5 times the inter-quartile range of the lower (upper) quartile. Values exceeding those whisker ends (minimum and maximum outliers) are not depicted in the graphs, yet their number m (of the total number n) is indicated at the bottom of each box as "n/m".

to the decoupled sub-canopy and fully coupled stages, because of the low total number of data and the occurrence of daytime Wa/Dc stages in early morning or late afternoon hours. Hence, a direct comparison of fluxes (and later concentration differences) for the three coupling stages was only possible at night, or between the Ds and Cs/C stage, as these major driving variables showed similar distributions over the investigated time periods. Daytime fluxes of F_{H_2O}, F_{CO_2}, F_{O_3}, F_{NO_2}, F_{NO}, $F_{NH_4^+,tot}$, and $F_{NO_3^-,tot}$ replicate the pattern described for global radiation, with less available energy during the Wa/Dc stage compared to Ds and Cs/C stages. As a consequence, upward directed fluxes (F_{H_2O}, F_{NO_2}) are smaller during Wa/Dc, and downward directed fluxes (F_{CO_2}, F_{O_3}, F_{NO}, $F_{NH_4^+,tot}$, $F_{NO_3^-,tot}$) are larger during Wa/Dc. While F_{H_2O} during night was close to zero and showed small dispersions for all coupling stages and both IOP's (Fig. 8a), F_{CO_2} was positive (upward) for both IOPs during night (Fig. 8b). However, when comparing fluxes of different coupling stages, they repeated the pattern of air temperature only in the summer period (IOP-2): lowest medians in Wa/Dc were associated with lowest air temperatures. F_{O_3} during night was more negative in the fall period than in the summer period (Fig. 8c), even though air temperatures were higher (by approx. 4 K) and relative humidity was lower (by approx. 12 %). During both IOPs, night-time F_{O_3} were approx. 50 % lower than daytime O_3 fluxes, which is due to stomata closing during night. However, $F_{O_3} \neq 0$ during night points to a strong non-stomatal component of O_3 uptake, as extensively described by Fowler et al. (2001). F_{NO_2} (measurements during IOP-2 only) showed small fluxes during night (Fig. 8d, right panel). Here, the median during Wa/Dc was lower than those during Ds and Cs/C regimes. However, F_{NO_2} was always significantly >0 (upward directed), indicating the strong (chemically induced) NO_2 source within the canopy. During Ds and Cs/C conditions, F_{NO_2} exceeded that NO_2 flux where coupling was (very) low by a factor of approx. 10. This strongly points to the fact that deep canopy mixing is necessary to export the soil emitted NO from the forest floor into the above canopy surface layer (oxidized by O_3 to NO_2 in the first half meter above the forest floor, cf. Fig. 6, top panel).

For NO, night-time fluxes at 32 m were indistinguishable from zero (Fig. 10e, right panel) and daytime NO fluxes were always negative (downward). Due to the non-turbulent regime during nighttime, biogenic emission of NO from soil will stop if the NO concentration in the soil air is similar to that NO concentration in the laminar/molecular layer above the soil surface. For adjacent layers, titration of NO by O_3 will dominate. Small – but downward directed – NO fluxes at 32 m during day are most likely resulting from the fact that in the middle of the forest canopy usually the minimum of the vertical NO distribution is observed (see Fig. 6, top panel). This is due to corresponding (very) long residence times which favor the nearly complete reaction with O_3 (being 10–100 times higher in concentration than NO). The NO flux then simply follows the NO concentration gradient between above and mid-canopy levels.

During IOP-2, in the afternoon (12:00–18:00), turbulent NO_2 fluxes measured by eddy-covariance technique at 32 m ranged between +0.5 and +1.8 nmol m^{-2} s^{-1}, i.e. the *Waldstein-Weidenbrunnen* spruce forest appeared as a significant NO_2 source during this time period. Without loss of generality, we may consider this flux just as a net NO_2 flux, namely as the result of a downward directed deposition flux (NO_2 uptake by spruce needles) and an upward directed flux (due to complete oxidation ($NO+O_3 \rightarrow NO_2+O$) of the NO, which is biogenic emitted from forest soil). Ignoring potential (very small) emission of NO_2 from spruce needles (Lerdau et al., 2000) and estimating the NO_2 exchange with the spruce needles to approx. -0.2 nmol m^{-2} s^{-1} (dynamic chamber studies during IOP-2 by Breuninger et al., 2011), the corresponding biogenic NO flux from the forest soil should then range between +0.3 and +1.6 nmol m^{-2} s^{-1}. From the results of Bargsten et al. (2010), where soil samples of the *Waldstein-Weidenbrunnen* site were quantified for their net potential NO soil emission, maximum soil NO emissions of +1.7 nmol m^{-2} s^{-1} were estimated for the conditions of IOP-2.

Both $F_{NH_4^+,tot}$ and $F_{NO_3^-,tot}$, which have only been measured during IOP-1 (Fig. 8d and e, left panels) showed small negative values, again with medians during Wa/Dc closer to zero than those during Ds and Cs/C regimes.

Turbulent and chemical time scales (according to Lenschow, 1982), as well as Damköhler numbers, have been determined for the above-canopy layer only and all data obtained between 06:00–12:00 have not been considered (s Sect. 3.3). During daytime, turbulent time scales (τ_{turb}) showed a distinctive pattern of higher medians for the decoupled conditions (Wa/Dc), when comparing different coupling stages (Fig. 9a, b). During night time a similar pattern of higher medians during Wa/Dc conditions can be found (limited by availability of data in certain classes). During IOP-1 and IOP-2, τ_{turb} was longer at night than at day for partly and fully coupled conditions. Chemical time scales (τ_{chem}), however, were fairly constant when comparing different coupling stages separately for day or night-time (Fig. 9c, d), yet slightly longer at night. When comparing the fall period (IOP-1, Fig. 9c) with the summer period (IOP-2, Fig. 9d), interquartile ranges of τ_{chem} were wider during fall, and τ_{chem} was also longer than during the summer period. Given the relatively constant behavior of τ_{chem}, corresponding Damköhler numbers ($DA = \tau_{turb}/\tau_{chem}$, Fig. 9e, f) reflect the daytime pattern already described for τ_{turb}, with higher medians for decoupled conditions (Wa/Dc). During night-time, medians are still highest for Wa/Dc stages, but dispersion is widest for the Cs/C stages of the summer period. Only during partly or fully coupled summer daytime conditions does part of the interquartile range of Damköhler

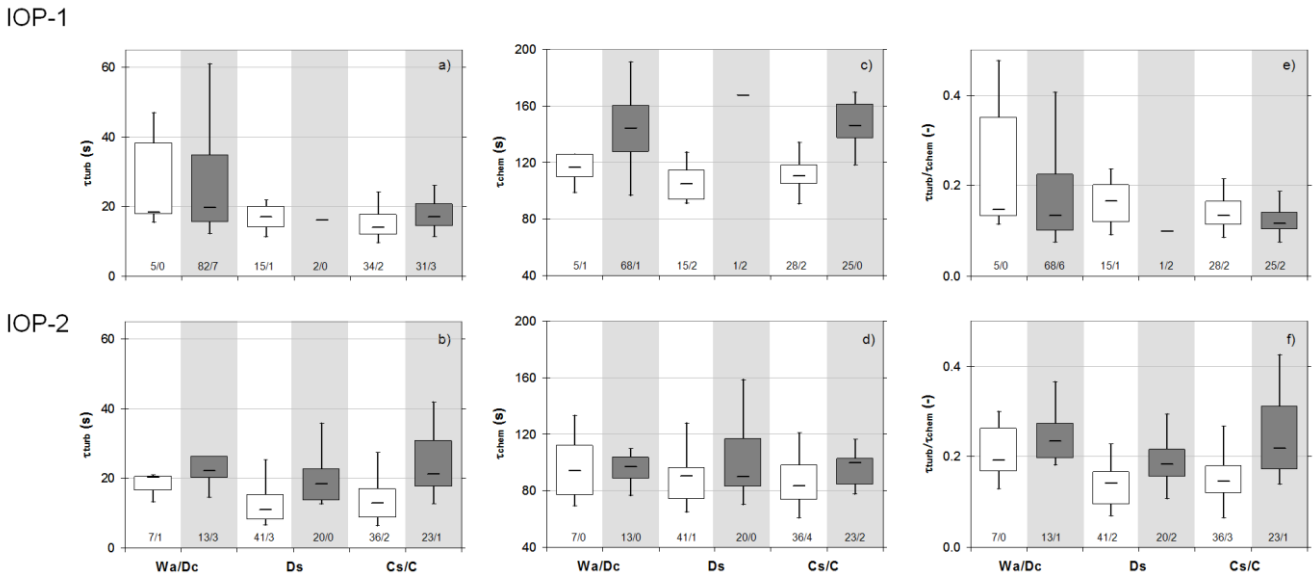

Fig. 9. Statistical dispersion and skewness of turbulent time scale τ_{turb} **(a, b)**, chemical time scale τ_{chem} **(c, d)**, and Damköhler number DA ($=\tau_{turb}/\tau_{chem}$; **e**, **f**) at the "main tower" for 20–24 September 2007 (IOP-1, DOY 263–267, top panels), and for 29 June to 2 July 2008 (IOP-2, DOY 181–184, bottom panels), classified by coupling regimes (Wa/Dc, decoupled conditions; Ds, decoupled subcanopy; Cs/C, coupled subcanopy by sweeps and fully coupled subcanopy) and day- (open box-plots) and night-time (grey shades). See also remarks on Fig. 8.

numbers fall below $DA < 0.1$ (i.e. where reactive trace gases may also be treated as "passive tracers"). Not surprising is that the turbulent time scales and Damköhler numbers for the coupling stages Ds and Cs/C are nearly identical. Both are determined above the canopy under coupled situation but in the case of Ds the forest floor is, of course, decoupled.

Further research is necessary to investigate whether the use of the turbulent time scale derived by the gradient approach (Mayer et al., 2011) is the appropriate method in cases when coherent structures dominate the flux. Therefore, the attempt should be made to detect coherent structures with a time scale less than 10 s, which is the lowest indicated duration for coherent structures applying the software used for this paper (Thomas and Foken, 2005). Consequently the duration time and the vertical scale of the structure should be used as the turbulent time scale for the Damköhler number. With such an approach Damköhler numbers may even be significantly below 0.1.

In summary – the size of fluxes and their standard deviations is similar for the coupled and partly coupled situations (Ds and Cs/c), but different for the non-coupled situations (Wa/Dc). For the latter case nearly no differences were observed between day and night, while for Ds and Cs/C stages significant differences were found. Both IOPs differ in the size of the fluxes and the distribution of the coupling stages according to Fig. 4. The Damköhler number is nearly similar for both IOPs because of shorter turbulent and chemical time scales in summer in relation to the fall experiment.

3.5 Concentration differences: top of canopy – forest floor

For the following analysis of vertical differences of trace gas concentrations, all data sets of measured concentration differences which have been obtained between 06:00–12:00 CET every day have been removed (see Sect. 3.3). During IOP-1, medians and interquartile ranges of H_2O concentration differences ($\Delta[H_2O] = [H_2O]_{24\,m} - [H_2O]_{0.9\,m}$) between the 24 and 0.9 m levels were always negative, indicating moister conditions below the canopy. A negative concentration difference (i.e. any quantity at the upper level is lower than the quantity at the lower level) corresponds to an upward directed vertical concentration gradient (away from the surface), while a downward directed vertical concentration gradient (to the surface) corresponds to a positive concentration difference. During IOP-2, night-time medians were positive, indicating drier below-canopy conditions compared to those above, whereas during the day mostly opposite gradients were observed (Fig. 10a).

For $\Delta[CO_2] = [CO_2]_{24\,m} - [CO_2]_{0.9\,m}$, medians and interquartile ranges were negative (upward directed gradient) but were, however, closer to zero during the day than during night (Fig. 10b). During daytime Wa/Dc regimes these negative CO_2 gradients were largest, again possibly due Wa/Dc stages close to night-time, with more pronounced CO_2 differences between top of canopy above and forest floor. Medians and inter-quartile ranges of $\Delta[O_3]$ were positive (downward directed gradient) for both periods, day- and night-time, and all coupling stages (Fig. 10c). However, during both IOPs

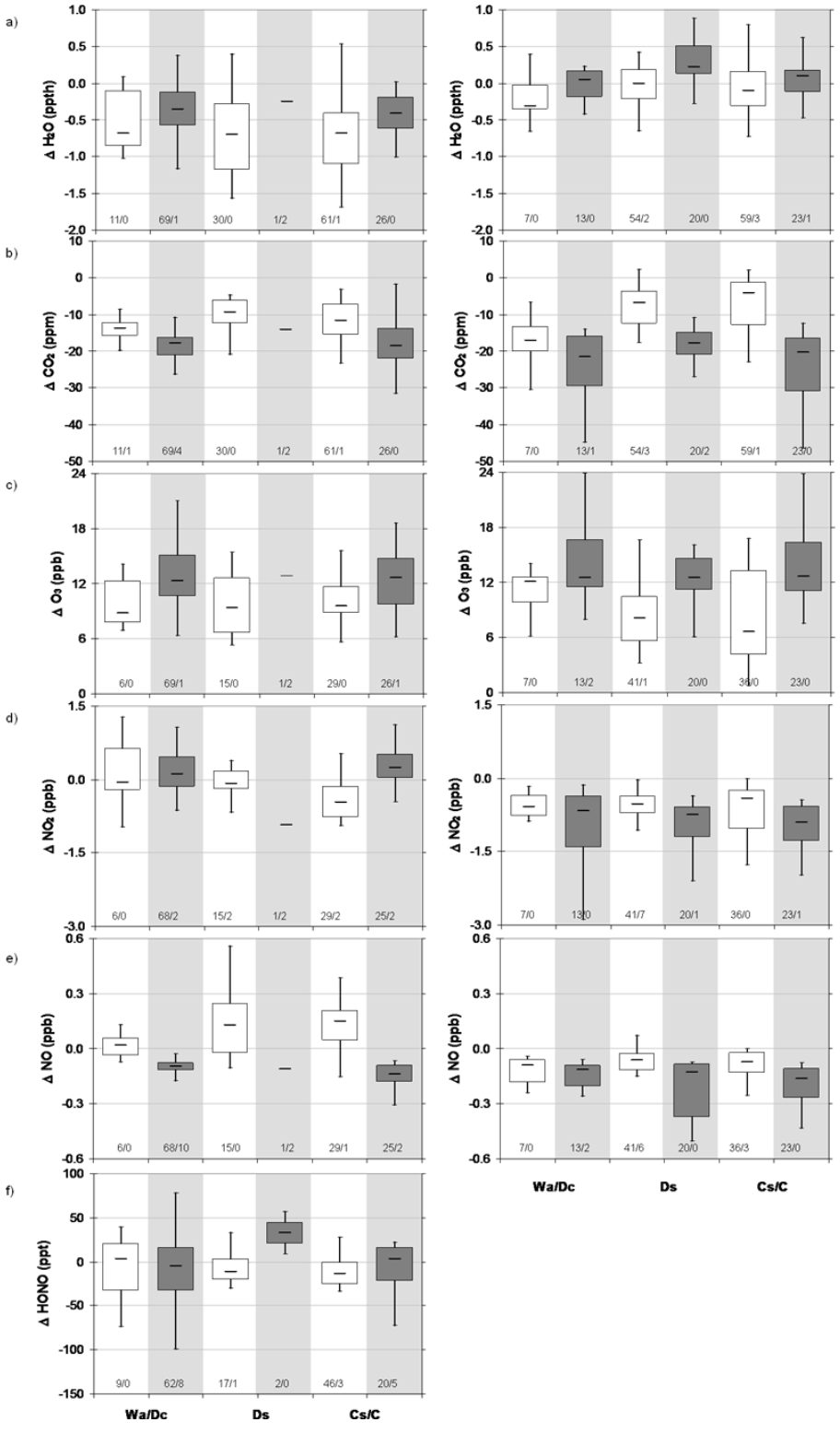

Fig. 10. Statistical dispersion and skewness of concentration differences Δ at the "main tower" for 20–24 September 2007 (IOP-1, DOY 263–267, left panels) and for 29 June to 2 July 2008 (IOP-2, DOY 181–184, right panels): ΔH_2O **(a)**, ΔCO_2 **(b)**, ΔO_3 **(c)**, ΔNO_2 **(d)**, ΔNO **(e)**, and ΔHONO (**f**, IOP-1 only). Data were classified by coupling regimes (Wa/Dc, decoupled conditions; Ds, decoupled subcanopy; Cs/C, coupled subcanopy by sweeps and fully coupled subcanopy) and day- (open box-plots) and night-time (grey shades). See also remarks on Fig. 8.

larger $\Delta[O_3]$'s were observed at night (medians > 12 ppb) as compared to daytime (medians < 12 ppb). In the fall period (IOP-1), $\Delta[NO_2] = [NO_2]_{24\,m} - [NO_2]_{0.9\,m}$ was negative during daytime for the Ds and Cs/C regimes, and positive or close to zero otherwise (Fig. 10d, left panel); during IOP-2 (summer) medians and inter-quartile ranges were clearly negative, with medians slightly more negative (up to -1.3 ppb) and larger inter-quartile ranges at night (Fig. 10d, right panel). Small negative medians of Δ[NO] were observed for most of the summer period (IOP-2) and during fall (IOP-1) at night-time hours (Fig. 10e). During hours where Ds and Cs/C prevailed, $\Delta[HONO] = [HONO]_{24\,m} - [HONO]_{0.9\,m}$ was negative during the daytime hours, and positive during much of the night (Fig. 10f). Under Wa/Dc regimes, medians of Δ[HONO] change sign (day: negative, night: positive), but also show much wider dispersion as indicated by the large inter-quartile range.

Any trial to synthesize Figs. 8 and 10 based on the common flux/gradient relationship $F = -v_{ex}\,[m(z_2) - m(z_1)]$, for $z_2 > z_1$ are flawed because fluxes F were measured in 32 m, while concentration differences Δm were evaluated between 24 and 0.9 m. Proportionality between the data shown in Figs. 8 (fluxes) and 10 (concentration differences) is therefore not expected. This may sound trivial at first glance, but has rather interesting implications. Comparing both figures, it is very remarkable that during IOP-1 and IOP-2 the signs of Δm and F for the examined scalars (H_2O, CO_2, O_3, NO_2, and NO) are always compatible under night-time conditions, and nearly always correspond under daytime conditions. That is, negative Δm concur with positive F, and positive Δm concur with negative F.

However there are two exceptions: negative daytime F_{NO} coincide with negative Δ[NO], and negative daytime F_{CO_2} coincide with negative $\Delta[CO_2]$, with the exception of Wa/Ds stages in IOP-2 (7 values only). What distinguishes daytime CO_2 and NO from the other scalars and from night-time conditions? The answer lies within the "control volume" (i.e. between $z = 0$ m and $z = 32$ m) for a flux measured at $z = 32$ m. Whereas for the sign-conforming cases (night-time conditions and daytime H_2O, O_3, and NO_2) the control volume contains either sources or sinks, for the non-conform scalars (daytime CO_2 and NO) the control volume contains both, sources as well as sinks for the respective scalar.

For daytime CO_2, the control volume contains CO_2 sources from soil, trunk and leaf respiration and the even stronger CO_2 sink, i.e. the assimilation by green leaves in understory and canopy. Hence, the mixture of biological sources and sinks within the control volume distorts the conformity between flux and concentration differences. This is completely different during the night, where the CO_2 sink term "assimilation" is missing, only source terms remain, and signs of flux and $\Delta[CO_2]$ are consistent again.

Now, for daytime NO, which is biogenic formed in the soil and emitted from the soil surface to the forest atmosphere, there are no known biological sinks in the control volume. However, most of the emitted NO is oxidized by O_3 to NO_2 in the first few tenths of a meter above the forest floor, and a part obviously also still above the first meter. The typical "back reaction", the photolysis of NO_2 to O_3 and NO, is suppressed, since it is comparatively dark below/within the canopy or in the understory. Most of the NO_2 (the former NO) can leave the control volume at $z = 32$ m, because the uptake by the needles is much lower than for O_3 (Breuninger et al., 2011; Geßler et al., 2002; Chaparro-Suarez et al., 2011). Hence, in the case of NO, the mixture of mainly biological sources and mainly chemical sinks within the control volume is responsible for the non-conformity between flux and concentration differences.

Regarding the HONO mixing ratio, differences for Ds and Cs/C regimes are very similar at daytime (slightly negative or close to zero), which could be attributed to good vertical mixing. At night time no clear result is visible due to the very limited number of measurements. Sörgel et al. (2011) concluded that differences in source and sink processes in and above the forest canopy became obvious only for the decoupled situations (Wa, Dc, Ds). Otherwise concentration differences were close to zero. The positive values during night could partly be attributed to advection of HONO rich air above the canopy which only partly penetrated the canopy.

In summary, the rather qualitative synopsis of Figs. 8 and 10 made the common problem of non-reactive as well as reactive trace gases evident, namely that a mixture of source and sink terms in the control volume of a flux requires careful assessment of primary sinks and sources, turbulence, and photochemical interactions. Corresponding questions are the subject of our ongoing analyses.

3.6 Modelling of fluxes

In this section modelling of fluxes is confined to that of energy fluxes, particularly to H_2O (latent heat) fluxes. This was just to study the basic performance of both applied model types, the agreement/non-agreement between the results of both models and between model and corresponding measurement results (H_2O eddy covariance). It should be noted, that ongoing model development aims corresponding studies concerning fluxes of (non-reactive) CO_2 and the reactive compounds NO, NO_2, O_3, and HONO.

For EGER IOP-1 campaign, H_2O (latent heat) exchange was analyzed with the three dimensional microclimate and gas exchange model STANDFLUX (Falge et al., 1997, 2000), as well with the one dimensional model ACASA (Pyles, 2000; Pyles et al., 2000). Both models were parameterized for the *Waldstein-Weidenbrunnen* site. Parameters common to both models included information on vertical leaf area distribution, and specific sets of physiological parameters for top, middle, and bottom canopy leaf gas exchange. STANDFLUX employed, in addition, horizontal leaf area distribution, tree positions and tree sizes. Further

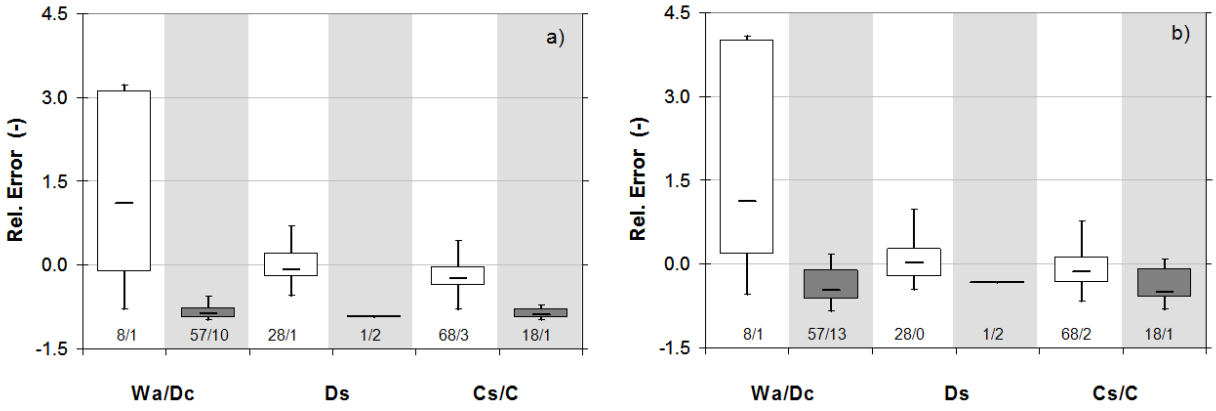

Fig. 11. Statistical dispersion and skewness of relative model error with respect to coupling stages from **(a)** STANDFLUX, and **(b)** ACASA; measured and modelled evapotranspiration data ranged from 20 through 24 September 2007 (IOP-1, DOY 263–267); measured evapotranspiration from turbulence tower 36 m level. Data were classified by coupling regimes (Wa/Dc, decoupled conditions; Ds, decoupled subcanopy; Cs/C, coupled subcanopy by sweeps and fully coupled subcanopy) and day- (open box-plots) and night-time (grey shades). See also remarks on Fig. 8.

information on model theory and setup is found in Staudt et al. (2011). H_2O exchange is modelled as the energy equivalent of the sum of evaporation from interception pools and upmost soil and litter layer, and tree and understory transpiration.

Prerequisite of comparisons between measured and modeled energy fluxes is a closed energy balance (Falge et al., 2005), because physical models are based on energy balance closure. In former studies, a value of 77 % (Aubinet et al., 2000; Foken, 2008b) was found. During both IOPs similar values were found with approx. 80 % for both IOP's (see Supplement).

Coupling state analysis of measured data and model predictions, based on Thomas and Foken (2007a), complement traditional analyses of data-model comparisons. Three coupling stages are distinguished: wave motion and decoupled canopy (code Wa/Dc, $n = 8$ during daytime, $n = 57$ during night-time), decoupled sub-canopy (code Ds, $n = 28$ during daytime, $n = 1$ during nighttime), coupled sub-canopy by sweeps and entirely coupled (code Cs/C, $n = 68$ during daytime, $n = 18$ during night-time). The use of coupling states demonstrates which turbulence stages are well represented and which are poorly represented by the model, and thus can serve as a diagnostic tool to improve turbulence parameterizations. By visualizing the data with respect to coupling stages, data-model mismatch at the different stages can be identified (see Fig. 11).

Figure 11 shows, that for the daytime decoupled cases (Wa/Dc), both models largely overestimated eddy-covariance measurements, probably resulting from the difficulties in performing eddy-covariance measurements under decoupled conditions. During daytime, STANDFLUX underestimates the measured evapotranspiration, especially for the Cs/C stage (Fig. 11a), when comparing the model results to the eddy covariance data from the turbulence tower at 36 m (Staudt et al., 2011). The performance of STANDFLUX improves when compared against eddy covariance data from the main tower at 32 m (data not shown), because the eddy covariance fluxes measured at the main tower are lower than those measured at the turbulence tower ($LE_{32\,m} = 0.92\ LE_{36\,m} - 8.8$, $r^2 = 0.88$, for 20–24 September 2007, and quality flags 1–6), potentially because the two towers sample different footprints. ACASA gave slightly better results compared to the measured evapotranspiration at Ds, and Cs/C stage (Fig. 11b). However, ACASA underestimates canopy transpiration (Staudt et al., 2011); an overestimation of evapotranspiration implies therefore an overestimation of the evaporation sources (soil and interception pool) by the model. For night-time conditions, both models underestimated eddy-covariance measurements during all coupling stages. Reasons for this underestimation might either originate in the models or the eddy-covariance measurements which might be underestimates themselves due to the lack of energy balance closure, exacerbating the underestimation of the models even more. Then again, the eddy-covariance estimates might be overestimating the uniform forest below the tower due to the contribution of clearings to the flux footprint. These clearings were found to act as a source of moisture and thus increase eddy-covariance estimates. The reasons for the modeled underestimation of eddy-covariance transpiration measurements are different for the two models ACASA and STANDFLUX. Ecosystem evapotranspiration modeled with the ACASA model agreed better with eddy-covariance measurements (Fig. 11b), but partly for the wrong reason: an overestimation of soil and understory evapotranspiration with a constant offset of about $10\,W\,m^{-2}$, compensated the modeled canopy transpiration which was too low. In contrast, the STANDFLUX model underestimated both, canopy transpiration and soil and understory evapotranspiration. However, it should be noted that, even though relative

errors of the models were large, absolute errors were only $8\,W\,m^{-2}$ for ACASA and $10\,W\,m^{-2}$ for STANDFLUX during decoupled conditions, and $15\,W\,m^{-2}$ for both models for coupled conditions.

High variances are expected because the dynamic footprint always adds to the flux variance at half-hourly time scales, that is, the eddy-covariance method does not sample the same patch all the time, whereas the model setup is static. In addition, the relative errors might show larger variances, because the models do not account for sweeps and ejections or for the conditions of the Wa stage, where neither the assumptions for the model nor for eddy-covariance theory are fulfilled. In the stable canopy space stimulation of gravity waves occurs at times (Cava et al., 2004; Lee et al., 1997). Under certain conditions, such waves become nonlinear and lead to ejections from the canopy (Fitzjarrald and Moore, 1990). Because of difficulties in resolving the Reynolds mean, effects of such singular events may be improperly calculated in a half-hourly eddy flux record.

4 Conclusions and outlook

It was the aim of the present exercise (a) to introduce the research of the two experimental events within the wider project EGER (ExchanGE processes in mountainous Regions), and (b) to present first results of above canopy exchange fluxes and concentration differences (top of canopy – forest floor) of non-reactive and reactive trace gases in relation to the turbulent coupling situations (between the above-canopy atmosphere and the canopy). Main results and findings are concluded as follows:

- It was important to complete the experimental EGER studies by boundary-layer profiling measurements, because boundary-layer phenomena also influence transport processes at the spatial scale of the field site. One of the most important phenomena in this respect is that of low-level jets, which may re-distribute vertical concentration profiles (see Fig. 6) and increase surface fluxes due to strong vertical shear. Similar effects may be caused by gravity waves. However, both phenomena are very much related to site-specific conditions. These situations are responsible for well-coupled situation (Cs/C) at night time where significant fluxes occur. In routine measuring programs such situations are not detected (due to the lack of necessary instrumentation), often deleted, and eventually gap filled according the friction velocity criterion (Goulden et al., 1996; Papale et al., 2006).

- The analysis of the coherent structures and coupling can be applied to an even wider range than shown above. The method of the analysis of coherent structures even offers the selection of sweeps and ejections in and above the canopy. Serafimovich et al. (2011) have shown that coupling is not only a vertical exchange effect but also a horizontal one. The horizontal coupling depends substantially on the canopy structure, which may be represented by sub-canopy density and the PAI. Therefore a careful analysis of both quantities is essential. This was applied by Siebicke (2011) to give a more general explanation of the night-time in-canopy CO_2-advection problem.

- By comparing the sign of fluxes and concentration differences (gradients), initially only done for H_2O and CO_2, fluxes show the expected diurnal cycle and are widely similar for all days. In contrast, concentration differences only follow these diurnal cycles for some selected periods and show a somewhat irregular pattern. This is a strong indication, that concentrations measured near the forest floor are decoupled from fluxes and concentrations measured above the canopy. Because the sign of the fluxes often disagrees with the direction of the gradient, counter gradient fluxes are apparent (Denmead and Bradley, 1985). Such situations are typically related to decoupled situations (Wa/Dc). Further analysis of such situations should be concentrate on indicators when potential forcing parameters, other than wind velocity and radiation, should be studied in detail.

- Quantitative analysis of fluxes (or concentration differences) with respect to coupling stages is, on one hand, limited by the small number of data points for some of the coupling stages (daytime Wa/Dc during IOP-1 and IOP-2, and night-time Ds during IOP-1). On the other hand, and even more importantly, coupling stages are subject to a typical diurnal and annual variation (see Fig. 4), and therefore superimposed by differences of meteorological quantities between the coupling stage categories (see Sect. 3.1). Therefore, differences in the magnitude of fluxes between the coupling stage classes may be mainly due to differences in available energy, atmospheric demand, or available soil water (in the case of F_{H_2O}), and only partially influenced by the coupling stage itself. Similarly, the magnitudes of F_{CO_2} (or F_{O_3}) may be modulated by the associated coupling stages, but certainly are driven by radiation, temperature and humidity, which affect stomatal opening (or chemical conversions) and consequently deposition velocities.

- Classification of the above canopy net NO_2 fluxes with respect to coupling stages revealed 10-fold higher fluxes for fairly and fully coupled conditions (Ds, Cs/C), compared to the decoupled conditions (Wa/Dc). This is a very clear indication that deep canopy mixing was necessary to export the soil emitted NO from the forest floor into the surface layer above the canopy.

- Despite the fact, that turbulent fluxes (measured at 32 m) can not directly related to corresponding concentration differences (evaluated between 24 and 0.9 m), the

comparison between both quantities clearly shows, that there are mainly negative concentration differences and positive fluxes (both upward directed) under night-time conditions, while during daytime mainly positive concentration differences are with negative fluxes (both downward directed). Considerable exceptions from this (expected) behaviour (i.e. fluxes of CO_2 and NO) make the common problem of non-reactive as well as reactive trace gases evident, namely the delicate mixture of sources and sinks in the control volume of a flux. Consequently, interpretation of above-canopy fluxes definitely requires careful assessment of primary sinks and sources, turbulence, and photochemical interactions.

– The diurnal evolution of HONO mixing ratio differences in and above the forest canopy could be well explained by the different source and sink processes (e.g. photolysis, heterogeneous formation and advection) in combination with the coupling regimes (see Sörgel et al., 2011). During periods of complete coupling (C and Cs cases), concentration differences were close to zero, despite large differences (factor 10 to 25) in the photolytic sink during daytime. During night-time, higher values above canopy could be partly be explained by advection of HONO rich air, whereas higher values below canopy in the afternoon (Ds, Wa/Dc) may point to a local source at the forest floor. In summary, the magnitude of concentration differences seems to be controlled by the amount of vertical mixing, whereas its sign by different source or sink processes.

– Keeping the uncertainties of the measurements in mind, the performance of the one-dimensional ACASA and the three-dimensional STANDFLUX models for H_2O exchange of the forest depends on the time of the day and the coupling conditions. Both models fall short of describing night-time evapotranspiration measurements, yet there is a better performance of the third-order closure model ACASA with an advanced representation of turbulence at night. Regardless of the individual model setup, i.e. three-dimensional versus one-dimensional representation of the stand, both model performances improved considerably during daytime, particularly for coupled and partly coupled situations.

– Coherent structures do not always follow the typical scaling system and this might increase turbulent mixing (Mahrt, 2010), which would consequently reduce the influence of fast chemical reactions to measured fluxes and concentration differences. First analysis of EGER data sets has already shown that the coupling concept (Thomas and Foken, 2007a) is without doubt a new and substantial tool for the interpretation of above-canopy fluxes and concentration differences (top of canopy versus forest floor). But it seems meaningful that the more point-related approach of the turbulent time scale (necessary for the calculation of the Damköhler number above the canopy) should be replaced by the spatio-temporal scale of coherent structures, which is based on the coupling concept. At least, this is definitely necessary when the contribution of coherent structures to vertical transport processes dominates (night time, see Figs. 8 to 11).

Finally, it should be emphasized that the investigation of the surface exchange of reactive trace gases, particularly those which are related to nearby anthropogenic (traffic) sources, could be strongly biased (if not endangered) by horizontal advection of temporally highly variable concentrations. Furthermore, there are different phenomena (LLJ, gravity waves) in the atmospheric boundary layer which might have drastic effects on the vertical distribution of non-reactive and reactive trace compounds and consequently on the observed exchange fluxes. Future field experiments should be designed such that these phenomena could be quantitatively considered, which may have decisive effects on above and in-canopy concentration profiles as well as exchange fluxes.

Appendix A

In-canopy plant and turbulence structure

Biometric data of the trees have been obtained by measurements of tree circumferences, tree positions (Forest Laser, Criterion Survey Laser Series 400, Laser Technology Inc., USA), and tree heights and crown lengths (inclinometer, Suunto, Finland). Horizontal distribution of Plant Area Index (PAI) was measured with two optical area meters (Plant Canopy Analyzer, LAI2000, LiCor, USA). The site inventory, available for the fenced area of the *Waldstein-Weidenbrunnen* site (1.3 ha), was used for the parameterization of the 3-D STANDFLUX model. The plant area index is $5.6 \pm 2.1\,m^2\,m^{-2}$ for the overstory trees (average and standard deviation of 532 measurements within the fenced area). The measured PAI was converted to LAI ($4.8\,m^2\,m^{-2}$) and SAI ($0.8\,m^2\,m^{-2}$) using allometric relations from inventory data gathered during IOP-1 and IOP-2 at the site. Two thirds of the fenced ground area is covered with bare litter or understory composed of mainly *Deschampsia flexuosa* and mosses, with an LAI of $0.5\,m^2\,m^{-2}$ and less. In the remaining third, open places with frequent sun spots are covered with *Picea abies* and *Vaccinium myrtillus*, with understory PAI of $3.5\,m^2\,m^{-2}$. The average vertical profile of the plant area index is given in Fig. A1 (average from 5 profile measurements).

The turbulence structure can typically be described with the so-called integral turbulence characteristics (normalized standard deviations), which are nearly constant (Panofsky and Dutton, 1984) or have a small sensitivity to stratification (for an overview see Foken, 2008a). While the profiles of the mean wind speed above a canopy are strongly affected

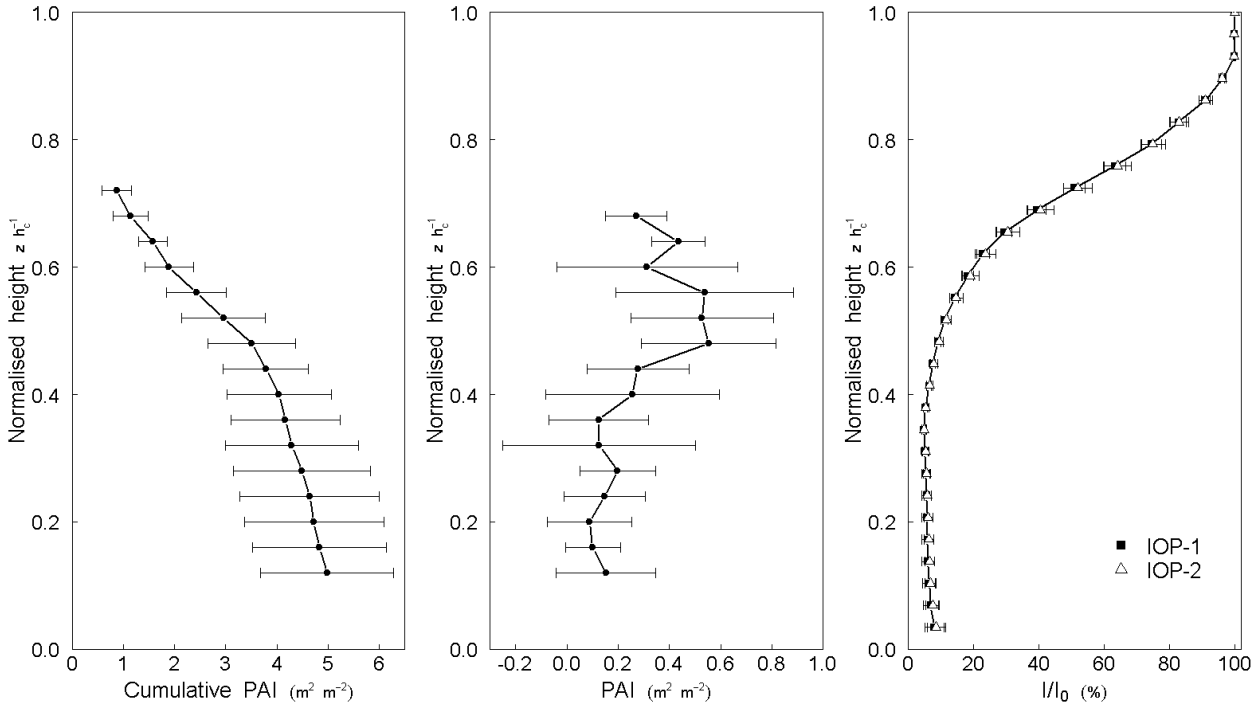

Fig. A1. Vertical profile of the (left) cumulative and (middle) absolute overstory plant area index (PAI) of the *Waldstein-Weidenbrunnen* site. Profiles are mean values of the five cumulative and absolute PAI profile measurements. Furthermore, the right figure shows the vertical distribution of the normalized shortwave radiation for both IOPs. The height is normalized by a canopy height of 25 m.

Table A1. Coefficients for Eq. (A1).

Reference	i	a_i	α_i	β_i	γ_i
Rannik et al. (2003), neutral, for *Hyytiäla* site	u	2.30	1.0	1.0	−0.3
	v	1.75	1.0	0.85	−0.2
	w	1.25	0.9	1.2	−0.63
Waldstein-Weidenbrunnen site, IOP-1	u	2.01	8.97	1.37	0.29
	v	1.60	5.18	1.11	0.34
	w	1.13	0.9	1.2	−0.63

by the existence of the roughness sublayer, the effect on integral characteristics is not well investigated and only a few investigations are available (Finnigan, 2000; Raupach et al., 1996). The turbulence characteristics within a forest are spatially heterogeneous and distinct from those associated with the surface boundary layer (Baldocchi and Meyers, 1998). For measurements inside the canopy ($z < h_c$) a parameterization was proposed by Rannik et al. (2003)

$$\frac{\sigma_i}{u_*} = a_i \left\{ \exp\left[-\alpha_i \left(1 - \frac{z}{h_c} \right)^{\beta_i} \right] (1-\gamma_i) + \gamma_i \right\} \qquad i = u, v, w;\ z < h_c \tag{A1}$$

and above the canopy constant values were assumed

$$\frac{\sigma_i}{u_*} = a_i \qquad i = u, v, w;\ z > h_c \tag{A2}$$

The values are given in Table A1. These are based on the measurements shown in Fig. A2.

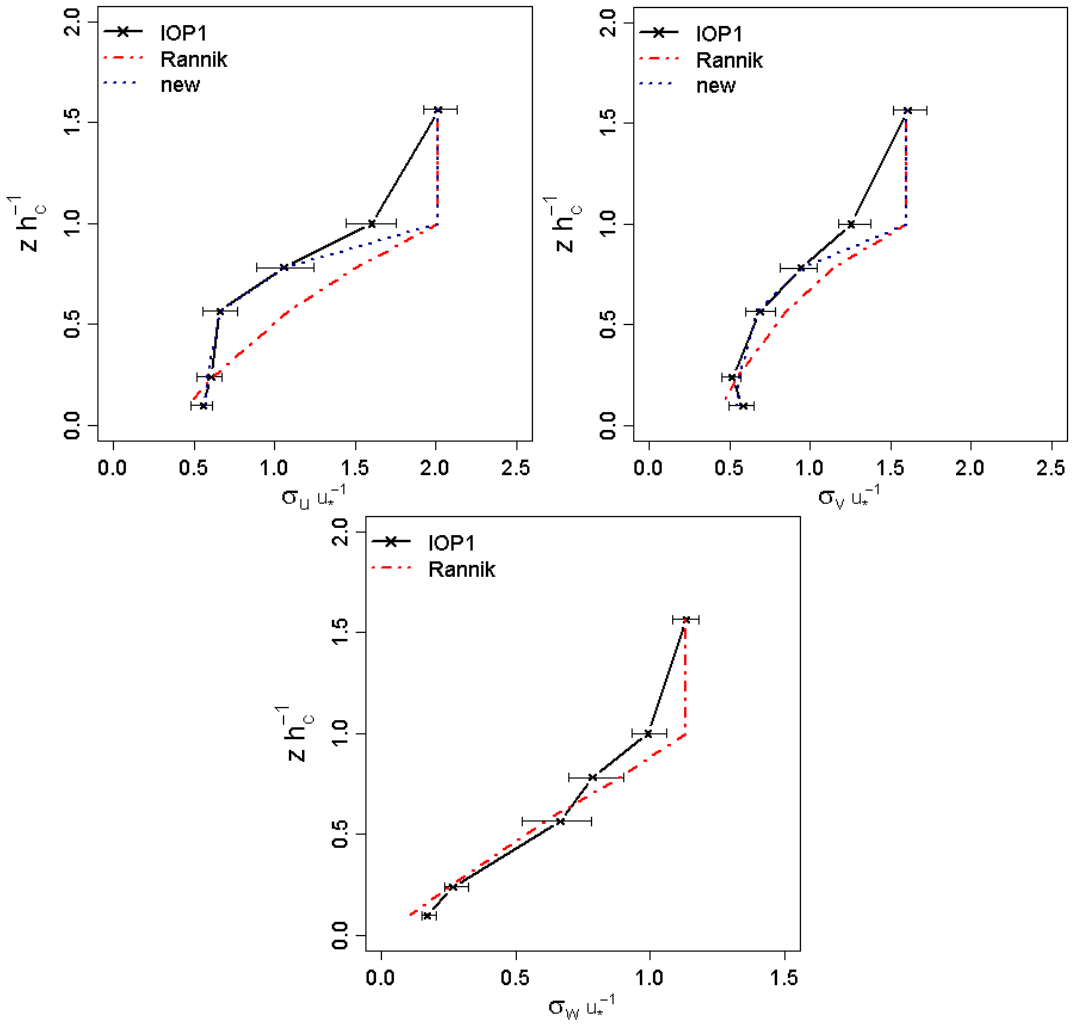

Fig. A2. Results of measurements (x, black line) and model parameterizations (red dot-dashed line) for profiles of the integral turbulence characteristics of wind velocity components u, v and w within the *Waldstein-Weidenbrunnen* forest stand and inside the lower roughness sublayer (near neutral stratification). For u and v the parameterization of Rannik et al. (2003) was modified to fit the measurements during IOP-1, for w the original coefficients were used.

Appendix B

The scale problem

The physical, chemical and biological processes which control the exchange of energy and trace substances are characterized by time scales extending from femto-seconds (e.g. electron transport in chloroplasts), over several hours (e.g. horizontal advection), to several years (climate, Benisston, 1998), and by spatial scales ranging from a few micrometers (e.g. reactions of heterogeneous chemistry) to the size of landscape elements (about $10 \times 10\,\mathrm{km}^2$). Investigations of the EGER project are focussing on widely overlapping scales (Jarvis, 1995) from contributions of the individual physical, chemical and biological processes, whereas our measuring and modelling techniques are related to specific scales.

The extent of the scale problem is illustrated in Fig. B1, where spatial and temporal scales of atmospheric, biological, soil and chemical processes, which control the exchange of energy and trace substances, are schematically shown. Within the entire range of atmospheric processes (light blue squares, ranging from micro scale γ to meso scale α, as defined by Orlanski, 1975), the scales concerning the exchange processes of energy, water, and trace substances comprise (i) turbulent transport in canopies, (ii) advection in canopies, (iii) turbulent transport above canopies, (iv) coherent structures in and above canopies, (v) footprint related turbulent fluxes, and (vi) horizontal advection at canopy top. In Fig. B1, the typical scales of processes in plants (Schoonmaker, 1998), those in soil (Vogel and Roth, 2003), in the saturated and unsaturated zone (Blöschl and Sivapalan, 1995) are shown by the brown framed, spotted area. While there

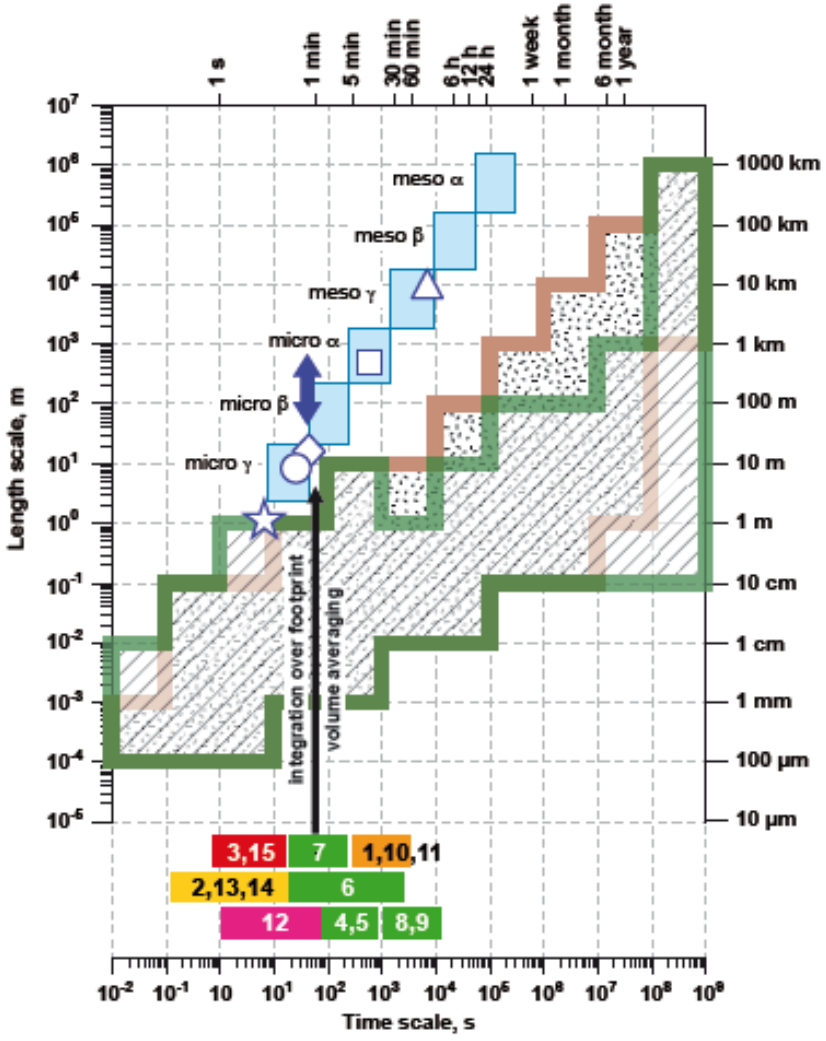

Fig. B1. Temporal and spatial scales of atmospheric, turbulent, plant, physiological, soil and relevant chemical processes forming the conceptual backbone of the EGER project. Atmospheric Processes (Orlanski, 1975) are given in light blue squares of one order of magnitude (from *micro* γ to *meso* α). Forest canopy related transport processes comprise turbulent transport in canopy (white star), vertical advection in canopy (white circle), transport above canopy (white diamond), coherent structures (blue double arrow), footprint averaged turbulent flux (white square), and horizontal advection at canopy top (white triangle). The scales of plant processes, relevant for energy and matter exchange with the atmosphere (Schoonmaker, 1998), those of soil processes are shown by the brown framed, spotted area (Vogel and Roth, 2003; Blöschl and Sivapalan, 1995). Time scales of relevant chemical reactions are shown according to Dlugi (1993, updated): (1) HO_2 + $HO_2 \rightarrow H_2O_2 + O_2$, (2) $HNO_3 + NH_3 \leftrightarrow NH_4NO_3$, (3) $O_3 + NO \rightarrow NO_2 + O_2$, (4) O_3 + isoprene $\rightarrow$ reaction products (P), (5) O_3 + monoterpenes $\rightarrow$ P, (6) NO_3 + monoterpenes $\rightarrow$ P, (7) NO_3 + isoprene $\rightarrow$ P, (8) OH + isoprene $\rightarrow$ R, (9) OH + monoterpenes $\rightarrow$ R, (10) O_3 + olefins $\rightarrow$ R, (11) $O_3 + NO_2 \rightarrow NO_3 + O_2$, (12) $N_2O_5 + H_2O \rightarrow 2HNO_3$, (13) HNO_3 $(+H_2O) \rightarrow H^+ + NO_3^-$, (14) $H_2O + 2NO_2$ (het) $\rightarrow HNO_2 + HNO_3$ (g), (15) $NO_2 + h\nu \rightarrow NO + O$ (for details of concentration ranges see Dlugi, 1993).

is a broad overlapping of the spatial and temporal scales of plant and soil processes, there is only a marginal overlapping of these with the scales of atmospheric processes; with increasing time scales, atmospheric processes separate more and more from plant and soil processes with regard to space. Not included in Fig. B1 are spatio-temporal scales of the measuring techniques from plant enclosures and soil chambers (a few tenths of square metres) to eddy-covariance data with a footprint up to some square kilometres. Remote sensing techniques have even larger areas, depending on the height from where the signal originates.

Note that coherent structures do not completely fulfil this picture of the atmospheric scales. They have a significantly larger length scale in the vertical than in the horizontal direction, and time scales are also longer. Therefore, they are able to couple even small special scales, which are typical in the biosphere with larger atmospheric scales. But also in horizontal direction a coupling over larger distances is possible

(Serafimovich et al., 2011). This important issue was recently underlined by Mahrt (2010) regarding the averaging technique for eddy-covariance measurements.

Gas-phase and heterogeneous reactions of relevant reactive trace gases (see reactions 1–15 in Fig. B1) are only attributed to corresponding temporal scales ($1/e$ reaction times). These characteristic chemical time scales (see Dlugi, 1993) simply result from ambient concentrations of the reaction partners, reaction kinetics or thermodynamic equilibrium considerations, and (photo-)chemical constants or variables. However, most of the corresponding (photo-)chemical constants have been derived from laboratory experiments in well-mixed reaction chambers (see Atkinson et al., 2004). Therefore, corresponding spatial scales (most likely $\ll$1 mm) seem not to be relevant for real atmospheric conditions, particularly not within tall canopies, where (strong) de-coupling by vertical thermodynamic stratification is (at least during night) more likely than full coupling with the (above canopy) surface layer, or even complete turbulent mixing throughout trunk and canopy spaces. The latter, however, is the prerequisite of corresponding volume averaging of chemical processes, which is a volume averaging of soil and plant processes – the basis of coupling of turbulent, soil, plant, and chemical processes.

Supplementary material related to this article is available online at: http://www.atmos-chem-phys.net/12/1923/2012/acp-12-1923-2012-supplement.pdf.

Acknowledgements. We are grateful for the support by the Bayreuth Center of Ecology and Environmental Research (BayCEER), mainly of G. Müller. Our thanks also go to J. Olesch and J. Sintermann for their support on the field site. We would also like to thank the Karlsruhe Institute of Technology and John Tenhunen (University of Bayreuth) for the support with measuring equipment and Ralph Dlugi, Bernd Huwe, Eberhard Schaller and Franz H. Berger for the intensive discussion during the preparation phase of the EGER project and especially for the development of the scale analysis.

The project was funded by the German Science foundation (DFG) under the contract numbers DFG projects: FO 226/16-1, ME 2100/4-1, ZE 792/4-1 and by the Max Planck Society. The continuously running meteorological systems were supported by the Oberfrankenstiftung e.V. under the contract number 01879. Analyses of the wet deposition were made by the Bavarian Environment Agency Augsburg and the chemical soil analysis by the Central Laboratory of BayCEER. The windprofiler data were kindly made available by the Richard-Aßmann-Observatory of the German Meteorological Service.

Edited by: T. Karl

References

Alaghmand, M., Shepson, P. B., Starn, T. K., Jobson, B. T., Wallace, H. W., Carroll, M. A., Bertman, S. B., Lamb, B., Edburg, S. L., Zhou, X., Apel, E., Riemer, D., Stevens, P., and Keutsch, F.: The morning NO_x maximum in the forest atmosphere boundary layer, Atmos. Chem. Phys. Discuss., 11, 29251–29282, doi:10.5194/acpd-11-29251-2011, 2011.

Amiro, B. D.: Comparison of turbulence statistics within three boreal forest canopies, Bound.-Lay. Meteorol., 51, 99–121, 1990.

Antonia, R. A.: Conditional sampling in turbulence measurements, Annu. Rev. Fluid Mech., 13, 131–156, 1981.

Arya, S. P.: Introduction to Micrometeorology, Academic Press, San Diego, 415 pp., 2001.

Atkinson, R., Baulch, D. L., Cox, R. A., Crowley, J. N., Hampson, R. F., Hynes, R. G., Jenkin, M. E., Rossi, M. J., and Troe, J.: Evaluated kinetic and photochemical data for atmospheric chemistry: Volume I – gas phase reactions of O_x, HO_x, NO_x and SO_x species, Atmos. Chem. Phys., 4, 1461–1738, doi:10.5194/acp-4-1461-2004, 2004.

Aubinet, M.: Eddy covariance CO_2 flux measurements in nocturnal conditions: An analysis of the problem, Ecol. Appl., 18, 1368–1378, 2008.

Aubinet, M., Grelle, A., Ibrom, A., Rannik, Ü., Moncrieff, J., Foken, T., Kowalski, A. S., Martin, P. H., Berbigier, P., Bernhofer, C., Clement, R., Elbers, J., Granier, A., Grünwald, T., Morgenstern, K., Pilegaard, K., Rebmann, C., Snijders, W., Valentini, R., and Vesala, T.: Estimates of the annual net carbon and water exchange of forests: The EUROFLUX methodology, Adv. Ecol. Res., 30, 113–175, 2000.

Aubinet, M., Heinesch, B., and Yernaux, M.: Horizontal and vertical CO_2 advection in a sloping forest, Bound.-Lay. Meteorol., 108, 397–417, 2003.

Aubinet, M., Feigenwinter, C., Heinesch, B., Bernhofer, C., Canepa, E., Lindroth, A., Montagnani, L., Rebmann, C., Sedlak, P., and van Gorsel, E.: Direct advection measurements do not help to solve the night-time CO_2 closure problem: Evidence from three different forests, Agr. Forest. Meteorol., 150, 655–664, 2010.

Baldocchi, D. and Meyers, T.: On using eco-physiological, micrometeorological and biogeochemical theory to evaluate carbon dioxide, water vapor and trace gas fluxes over vegetation, Agr. Forest. Meteorol., 90, 1–25, 1998.

Baldocchi, D., Falge, E., Gu, L., Olson, R., Hollinger, D., Running, S., Anthoni, P., Bernhofer, C., Davis, K., Evans, R., Fuentes, J., Goldstein, A., Katul, G., Law, B., Lee, X. H., Malhi, Y., Meyers, T., Munger, W., Oechel, W., PawU, K. T., Pilegaard, K., Schmid, H. P., Valentini, R., Verma, S., and Vesala, T.: FLUXNET: A new tool to study the temporal and spatial variability of ecosystem-scale carbon dioxide, water vapor, and energy flux densities, B. Am. Meteorol. Soc., 82, 2415–2434, 2001.

Banta, R. M., Newsom, R. K., Lundquist, J. K., Pichugina, Y. L., Coulter, R. L., and Mahrt, L.: Nocturnal low-level jet characteristics over Kansas during Cases-99, Bound.-Lay. Meteorol., 105, 221–252, 2002.

Bargsten, A., Falge, E., Pritsch, K., Huwe, B., and Meixner, F. X.: Laboratory measurements of nitric oxide release from forest soil with a thick organic layer under different understory types, Biogeosciences, 7, 1425–1441, doi:10.5194/bg-7-1425-2010, 2010.

Beniston, M.: From turbulence to climate, Springer, Berlin,

Heidelberg, 328 pp., 1998.
Bergström, H. and Högström, U.: Turbulent exchange above a pine forest. II. Organized structures, Bound.-Lay. Meteorol., 49, 231–263, 1989.
Blöschl, G. and Sivapalan, M.: Scale issues in hydrological modelling – a review, Hydrol. Process., 9, 251–290, 1995.
Breuninger, C., Oswald, R., Kesselmeier, J., and Meixner, F. X.: The dynamic chamber method: trace gas exchange fluxes (NO, NO_2, O_3) between plants and the atmosphere in the laboratory and in the field, Atmos. Meas. Tech. Discuss., 4, 5183–5274, doi:10.5194/amtd-4-5183-2011, 2011.
Businger, J. A.: Evaluation of the accuracy with which dry deposition can be measured with current micrometeorological techniques, J. Appl. Meteorol., 25, 1100–1124, 1986.
Cava, D., Giostra, U., Siqueira, M., and Katul, G.: Organised motion and radiative perturbations in the nocturnal canopy sublayer above an even-aged pine forest, Bound.-Lay. Meteorol., 112, 129–157, 2004.
Chaparro-Suarez, I. G., Meixner, F. X., and Kesselmeier, J.: Nitrogen dioxide (NO_2) uptake by vegetation controlled by atmospheric concentrations and plant stomatal aperture, Atmos. Environ., 45, 5742–5750, 2011.
Collatz, G. J., Ball, J. T., Grivet, C., and Berry, J. A.: Regulation of stomatal conductance and transpiration, a physiological model of canopy processes, Agr. Forest. Meteorol., 54, 107–136, 1991.
Collineau, S. and Brunet, Y.: Detection of turbulent coherent motions in a forest canopy. Part II: Time-scales and conditional averages, Bound.-Lay. Meteorol., 66, 49–73, 1993a.
Collineau, S. and Brunet, Y.: Detection of turbulent coherent motions in a forest canopy. Part I: Wavelet analysis, Bound.-Lay. Meteorol., 65, 357–379, 1993b.
Damköhler, G.: Der Einfluss der Turbulenz auf die Flammengeschwindigkeit in Gasgemischen, Z. Elektrochem., 46, 601–652, 1940.
Denmead, D. T. and Bradley, E. F.: Flux-gradient relationships in a forest canopy, in: The forest-atmosphere interaction, edited by: Hutchison, B. A. and Hicks, B. B., D. Reidel Publ. Comp., Dordrecht, Boston, London, 421–442, 1985.
Dlugi, R.: Interaction of NO_x and VOC's within vegetation, in: Proceedings EUROTRAC-Symposium 92, edited by: Borrell, P. W., SPB Acad. Publ., The Hague, 682–688, 1993.
Falge, E., Tenhunen, J. D., Ryel, R., Alsheimer, M., and Köstner, B.: Modelling age- and density-related gas exchange of Picea abies canopies of the Fichtelgebirge, Germany, Ann. Sci. For., 57, 229–243, 2000.
Falge, E., Reth, S., Brüggemann, N., Butterbach-Bahl, K., Goldberg, V., Oltchev, A., Schaaf, S., Spindler, G., Stiller, B., Queck, R., Köstner, B., and Bernhofer, C.: Comparison of surface energy exchange models with eddy flux data in forest and grassland ecosystems of Germany, Ecol. Mod., 188, 174–216, 2005.
Falge, E. M., Ryel, R. J., Alsheimer, M., and Tenhunen, J. D.: Effects on stand structure and physiology on forest gas exchange: A simulation study for Norway spruce, Trees, 11, 436–448, 1997.
Farmer, D. K. and Cohen, R. C.: Observations of HNO_3, $\sum$AN, $\sum$PN and NO_2 fluxes: evidence for rapid HO_x chemistry within a pine forest canopy, Atmos. Chem. Phys., 8, 3899–3917, doi:10.5194/acp-8-3899-2008, 2008.
Farquhar, G. D. and von Caemmerer, S.: Modeling photosynthetic response to environmental conditions, in: Encyclopia of plant physiology II, 12b, edited by: Lange, O. L., Nobel, P. S., Osmond, C. B., and Ziegler, H., Springer, Berlin, 1982.
Feigenwinter, C., Bernhofer, C., Eichelmann, U., Heinesch, B., Hertel, M., Janous, D., Kolle, O., Lagergren, F., Lindroth, A., Minerbi, S., Moderow, U., Mölder, M., Montagnani, L., Queck, R., Rebmann, C., Vestin, P., Yernaux, M., Zeri, M., Ziegler, W., and Aubinet, M.: Comparison of horizontal and vertical advective CO_2 uxes at three forest sites, Agr. Forest. Meteorol., 148, 12–24, 2008.
Finnigan, J.: Turbulence in plant canopies, Annu. Rev. Fluid Mech., 32, 519–571, 2000.
Finnigan, J.: An introduction to flux measurements in diffiult conditions, Ecol. Appl., 18, 1340–1350, 2008.
Fitzjarrald, D. R. and Moore, K. E.: Mechanisms of nocturnal exchange between the rain forest and the atmosphere, J. Geophys. Res., 95, 16839–16850, 1990.
Foken, T.: Micrometeorology, Springer, Berlin, Heidelberg, 308 pp., 2008a.
Foken, T.: The energy balance closure problem – An overview, Ecol. Appl., 18, 1351–1367, 2008b.
Foken, T. and Leclerc, M. Y.: Methods and limitations in validation of footprint models, Agr. Forest. Meteorol., 127, 223–234, 2004.
Foken, T. and Wichura, B.: Tools for quality assessment of surface-based flux measurements, Agr. Forest. Meteorol., 78, 83–105, 1996.
Foken, T., Göckede, M., Mauder, M., Mahrt, L., Amiro, B. D., and Munger, J. W.: Post-field data quality control, in: Handbook of Micrometeorology: A Guide for Surface Flux Measurement and Analysis, edited by: Lee, X., Massman, W. J., and Law, B., Kluwer, Dordrecht, 181–208, 2004.
Fowler, D., Flechard, C., Cape, J. N., Storeton-West, R., and Coyle, M.: Measurements of ozone deposition to vegetation quantifying the flux, the stomatal and non-stomatal components, Water Air Soil Pollut., 130, 63–74, 2001.
Frankenberger, E.: Untersuchungen über den Vertikalaustausch in den unteren Dekametern der Atmosphäre, Ann. Meteorol., 4, 358–374, 1951.
Ganzeveld, L. N., Lelieveld, J., Dentener, F. J., Krol, M. C., Bowman, A. J., and Roelofs, G. J.: Global soilbiogenic emissions and the role of canopy processes, J. Geophys. Res., 107, 4298, doi:10.1029/2001JD001289, 2002.
Garratt, J. R.: Flux profile relations above tall vegetation, Q. J. Roy. Meteorol. Soc., 104, 199–211, 1978.
Garratt, J. R.: Surface influence upon vertical profiles in the atmospheric near surface layer, Q. J. Roy. Meteorol. Soc., 106, 803–819, 1980.
Gerstberger, P., Foken, T., and Kalbitz, K.: The Lehstenbach and Steinkreuz chatchments in NE Bavaria, Germany, in: Biogeochemistry of Forested Catchments in a Changing Enivironment, A German Gase Study. Ecological Studies, edited by: Matzner, E., Springer, Heidelberg, 15–41, 2004.
Geßler, A., Rienks, M., and Rennenberg, H.: Stomatal uptake and cuticular adsorption contribute to dry deposition of NH_3 and NO_2 to needles of adult spruce (Picea abies) trees, New Phytol., 156, 179–194, doi:10.1046/j.1469-8137.2002.00509.x, 2002.
Göckede, M., Rebmann, C., and Foken, T.: A combination of quality assessment tools for eddy covariance measurements with footprint modelling for the characterisation of complex sites, Agr. Forest. Meteorol., 127, 175–188, 2004.

Göckede, M., Markkanen, T., Hasager, C. B., and Foken, T.: Update of a footprint-based approach for the characterisation of complex measuring sites, Bound.-Lay. Meteorol., 118, 635–655, 2006.

Göckede, M., Thomas, C., Markkanen, T., Mauder, M., Ruppert, J., and Foken, T.: Sensitivity of Lagrangian Stochastic footprints to turbulence statistics, Tellus, 59B, 577–586, 2007.

Goulden, M. L., Munger, J. W., Fan, F.-M., Daube, B. C., and Wofsy, S. C.: Measurements of carbon sequestration by long-term eddy covariance: method and critical evaluation of accuracy, Glob. Change Biol., 2, 159–168, 1996.

Griffith, D. W. T., Leuning, R., Denmead, O. T., and Jamie, I. M.: Air-land exchanges of CO_2, CH_4 and N_2O measured by FTIR spectrometry and micrometeorological techniques, Atmos. Environ., 36, 1833–1842, 2002.

Güsten, H. and Heinrich, G.: On-line measurements of ozone surface fluxes: Part I. Methodology and instrumentation, Atmos. Environ., 30, 897–909, 1996.

Harman, I. N. and Finnigan, J. J.: A simple unified theory for flow in the canopy and roughness sublayer, Bound.-Lay. Meteorol., 123, 339–363, 2007.

Harman, I. N. and Finnigan, J. J.: Scalar concentration profiles in the canopy and roughness sublayer, Bound.-Lay. Meteorol., 129, 323–351, 2008.

Heland, J., Kleffmann, J., Kurtenbach, R., and Wiesen, P.: A new instrument to measure gaseous nitrous acid (HONO) in the atmosphere, Environ. Sci. Technol., 35, 3207–3012, 2001.

Horii, C. P., Munger, J. W., Wofsy, S., Zahniser, M., Nelson, D., and McManus, J. B.: Fluxes of nitrogen oxides over a temperate deciduous forest, J. Geophys. Res., 109, D08305, doi:10.1029/2003JD004326, 2004.

Jarvis, P. G.: Scaling processes and problems, Plant Cell Environ., 18, 1079–1089, 1995.

Karipot, A., Leclerc, M. Y., Zhang, G., Martin, T., Starr, D., Hollinger, D., McCaughey, H., and Hendrey, G. M.: Nocturnal CO_2 exchange over tall forest canopy associated with intermittent low-level jet activity, Theor. Appl. Climatol., 85, 243–248, 2006.

Karipot, A., Leclerc, M. Y., Zhang, G., Lewin, K. F., Nagy, J., Hendrey, G. R., and Starr, D.: Influence of nocturnal low-level jet on turbulence structure and CO_2 flux measurements over a forest canopy, J. Geophys. Res., 113, D10102, doi:10.1029/2007JD009149, 2008.

Karl, T., Harley, P., Emmons, L., Thornton, B., Guenther, A., Basu, C., Turnipseed, A., and Jardine, K.: Efficient atmospheric cleansing of oxidized organic trace gases by vegetation, Science, 330, 816–818, 2010.

Katul, G., Kuhn, G., Schieldge, J., and Hsieh, C.-I.: The ejection-sweep character of scalar fluxes in the unstable surface layer, Bound.-Lay. Meteorol., 83, 1–26, 1997.

Kleffmann, J., Heland, J., Lörzer, J. C., and Wiesen, P.: A new instrument (LOPAP) for the detection of nitrous acid (HONO), Environ. Sci. Pollut. Res., 9, 48–54, 2002.

Lee, X.: On micrometeorological observations of surface-air exchange over tall vegetation, Agr. Forest. Meteorol., 91, 39–49, 1998.

Lee, X., Neumann, H. H., Den Hartog, G., Fuentes, J. D., Black, T. A., Mickle, R. E., Yang, P. C., and Blanken, P. D.: Observation of gravity waves in a boreal forest, Bound.-Lay. Meteorol., 84, 383–398, 1997.

Lenschow, D. H.: Reactive trace species in the boundary layer from a micrometeorological perspective, J. Meteorol. Soc. Jpn., 60, 472–480, 1982.

Lerdau, M. T., Munger, J. W., and Jacob, D. J.: The NO_2 flux conundrum, Science, 289, 2291–2293, 2000.

Leuning, R. F. M.: Modeling stomatal behavior and photosynthesis of Eucalyptus grandis, Austr. J. Plant Physiol., 17, 159–175, 1990.

Mahrt, L.: Computing turbulent fluxes near the surface: Needed improvements, Agr. Forest. Meteorol., 150, 501–509, 2010.

Mauder, M. and Foken, T.: Documentation and instruction manual of the eddy covariance software package TK2, Arbeitsergebn., Univ. Bayreuth, Abt. Mikrometeorol., ISSN: 1614-89166, 26, 42 pp., 2004.

Mauder, M. and Foken, T.: Documentation and instruction manual of the eddy covariance software package TK3, Arbeitsergebn., Univ. Bayreuth, Abt. Mikrometeorol., ISSN: 1614-89166, 46, 58 pp., 2011.

Mauder, M., Foken, T., Clement, R., Elbers, J. A., Eugster, W., Grnwald, T., Heusinkveld, B., and Kolle, O.: Quality control of CarboEurope flux data – Part 2: Inter-comparison of eddy-covariance software, Biogeosciences, 5, 451–462, doi:10.5194/bg-5-451-2008, 2008.

Mayer, J. C., Bargsten, A., Rummel, U., Meixner, F. X., and Foken, T.: Distributed Modified Bowen Ratio method for surface layer fluxes of reactive and non-reactive trace gases, Agr. Forest. Meteorol., 151, 655–668, 2011.

Meixner, F. X., Andreae, M. O., van Dijk, S. M., Gut, A., Rummel, U., Scheibe, M., and Welling, M.: Biosphere-atmosphere exchange of reactive trace gases in a primary rainforest ecosystem: studies on interlinking scales, Rep. Ser. Aerosol Sci., 62A, 269–274, 2003.

Meyers, T. P.: A simulation of the canopy microenvironment using higher order closure principles, Ph.D. thesis, Purdue University, Purdue, 153 pp., 1985.

Meyers, T. P. and Paw U, K. T.: Testing a higher-order closure model for modelling airflow within and above plant canopies, Bound.-Lay. Meteorol., 37, 297–311, 1986.

Meyers, T. P. and Paw U, K. T.: Modelling the plant canopy microenvironment with higher-order closure principles, Agr. Forest. Meteorol., 41, 143–163, 1987.

Mölder, M., Grelle, A., Lindroth, A., and Halldin, S.: Flux-profile relationship over a boreal forest – roughness sublayer correction, Agr. Forest. Meteorol., 98–99, 645–648, 1999.

Monteith, J. L. and Unsworth, M. H.: Principles of environmental physics, 3rd edition, Elsevier, Academic Press, Amsterdam, Boston, 418 pp., 2008.

Mozurkewich, M.: The dissociation constant of ammonium nitrate and its dependence on temperature, relative humidity and particle size, Atmos. Environ. A-Gen., 27, 261–270, 1993.

Nenes, A., Pandis, S. N., and Pilinis, C.: ISORROPIA: A new thermodynamic equilibrium model for multiphase multicomponent inorganic aerosols, Aquat. Geochem., 4, 123–152, 1998.

Orlanski, I.: A rational subdivision of scales for atmospheric processes, B. Am. Meteorol. Soc., 56, 527–530, 1975.

Panofsky, H. A. and Dutton, J. A.: Atmospheric Turbulence – Models and methods for engineering applications, John Wiley and Sons, New York, 397 pp., 1984.

Papale, D., Reichstein, M., Aubinet, M., Canfora, E., Bernhofer, C.,

Kutsch, W., Longdoz, B., Rambal, S., Valentini, R., Vesala, T., and Yakir, D.: Towards a standardized processing of Net Ecosystem Exchange measured with eddy covariance technique: algorithms and uncertainty estimation, Biogeosciences, 3, 571–583, doi:10.5194/bg-3-571-2006, 2006.

Paw U, K. T. and Gao, W.: Application of solutions to non-linear energy budget equations, Agr. Forest. Meteorol., 43, 121–145, 1988.

Pryor, S. C., Larsen, S. E., Soerensen, L. L., Barthelmie, R. J., Groenholm, T., Kulmala, M., Launiainen, S., Rannik, U., and Vesala, T.: Particle fluxes over forests: Analyses of flux methods and functional dependencies, J. Geophys. Res., 112, D07205, doi:07210.01029/02006JD008066, 2007.

Pyles, R. D.: The development and testing of the UCD advanced canopy-atmosphere-soil algorithm (ACASA) for use in climate prediction and field studies, University of California, University of California, Davis, 194 pp., 2000.

Pyles, R. D., Weare, B. C., and Paw U, K. T.: The UCD Advanced Canopy-Atmosphere-Soil Algorithm: comparisons with observations from different climate and vegetation regimes, Q. J. Roy. Meteorol. Soc., 126, 2951–2980, 2000.

Rannik, U., Markkanen, T., Raittila, T., Hari, P., and Vesala, T.: Turbulence statistics inside and above forest: Influence on footprint prediction, Bound.-Lay. Meteorol., 109, 163–189, 2003.

Raupach, M. R. and Thom, A. S.: Turbulence in and above plant canopies, Annu. Rev. Fluid Mech., 13, 97–129, 1981.

Raupach, M. R., Finnigan, J. J., and Brunet, Y.: Coherent eddies and turbulence in vegetation canopies: the mixing-layer analogy, Bound.-Lay. Meteorol., 78, 351–382, 1996.

Rummel, U., Ammann, C., Gut, A., Meixner, F. X., and Andreae, M. O.: Eddy covariance measurements of nitric oxide flux within an Amazonian rainforest, J. Geophys. Res., 107, 8050, doi:10.1029/2001JD000520, 2002.

Schoonmaker, P. K.: Paleoecological perspectives on ecological scales, in: Ecological Scale, edited by: Peterson, D. L. and Parker, V. T., Columbia University Press, New York, 79–103, 1998.

Serafimovich, A., Siebicke, L., Staudt, K., Lüers, J., Biermann, T., Schier, S., Mayer, J.-C., and Foken, T.: ExchanGE processes in mountainous Regions (EGER): Documentation of the Intensive Observation Period (IOP1), September, 6 to 7 October 2007, Arbeitsergebn., Univ. Bayreuth, Abt. Mikrometeorol., ISSN: 1614-89166, 36, 145 pp., 2008a.

Serafimovich, A., Siebicke, L., Staudt, K., Lüers, J., Hunner, M., Gerken, T., Schier, S., Biermann, T., Rütz, F., Buttlar, J. v., Riederer, M., Falge, E., Mayer, J.-C., and Foken, T.: ExchanGE processes in mountainous Regions (EGER): Documentation of the Intensive Observation Period (IOP2) 1 June to 15 July 2008, Arbeitsergebn., Univ. Bayreuth, Abt. Mikrometeorol., ISSN: 1614-89166, 37, 180 pp., 2008b.

Serafimovich, A., Thomas, C., and Foken, T.: Vertical and horizontal transport of energy and matter by coherent motions in a tall spruce canopy, Bound.-Lay. Meteorol., 140, 429–451, doi:10.1007/s10546-011-9619-z, 2011.

Shaw, R. H.: Secondary wind speed maxima inside plant canopies, J. Appl. Meteorol., 16, 514–521, 1977.

Siebicke, L.: Footprint synthesis for the FLUXNET site Waldstein/Weidenbrunnen (DE-Bay) during the EGER experiment, Arbeitsergebn., Univ. Bayreuth, Abt. Mikrometeorol., ISSN: 1614-89166, 38, 45 pp., 2008.

Siebicke, L.: Advection at a forest site – an updated approach, Ph.D. thesis, University of Bayreuth, Bayreuth, 113 pp., 2011.

Siebicke, L., Hunner, M., and Foken, T.: Aspects of CO_2-advection measurements, Theor. Appl. Climatol., online first, doi:10.1007/s00704-011-0552-3, 2011a.

Siebicke, L., Steinfeld, G., and Foken, T.: CO_2-gradient measurements using a parallel multi-analyzer setup, Atmos. Meas. Tech., 4, 409–423, doi:10.5194/amt-4-409-2011, 2011b.

Smirnova, T. G., Brown, J. M., and Benjamin, S. G.: Performance of different soil model configurations in simulating ground surface temperature and surface fluxes, Mon. Weather Rev., 125, 1870–1884, 1997.

Smirnova, T. G., Brown, J. M., Benjamin, S. G., and Kim, D.: Parameterization of cold-season processes in the MAPS land-surface scheme, J. Geophys. Res., 105, 4077–4086, 2000.

Sörgel, M., Trebs, I., Serafimovich, A., Moravek, A., Held, A., and Zetzsch, C.: Simultaneous HONO measurements in and above a forest canopy: influence of turbulent exchange on mixing ratio differences, Atmos. Chem. Phys., 11, 841–855, doi:10.5194/acp-11-841-2011, 2011.

Staudt, K. and Foken, T.: Documentation of reference data for the experimental areas of the Bayreuth Centre for Ecology and Environmental Research (BayCEER) at the Waldstein site, Arbeitsergebn., Univ. Bayreuth, Abt. Mikrometeorol., ISSN: 1614-89166, 35, 35 pp., 2007.

Staudt, K., Serafimovich, A., Siebicke, L., Pyles, R. D., and Falge, E.: Vertical structure of evapotranspiration at a forest site (a case study), Agr. Forest. Meteorol., 151, 709–729, 2011.

Steiner, A. L., Pressley, S. N., Botros, A., Jones, E., Chung, S. H., and Edburg, S. L.: Analysis of coherent structures and atmosphere-canopy coupling strength during the CABINEX field campaign, Atmos. Chem. Phys., 11, 11921–11936, doi:10.5194/acp-11-11921-2011, 2011.

Stelson, A. W. and Seinfeld, J. H.: Relative-humidity and temperature-dependence of the ammonium-nitrate dissociation-constant, Atmos. Environ., 16, 983–992, 1982.

Stull, R. B.: An Introduction to Boundary Layer Meteorology, Kluwer Acad. Publ., Dordrecht, Boston, London, 666 pp., 1988.

Su, H.-B., Paw U, K. T., and Shaw, R. H.: Development of a coupled leaf and canopy model for the simulation of plant-atmosphere interactions, J. Appl. Meteorol., 35, 733–748, 1996.

Thomas, C. and Foken, T.: Detection of long-term coherent exchange over spruce forest, Theor. Appl. Climatol., 80, 91–104, 2005.

Thomas, C. and Foken, T.: Organised motion in a tall spruce canopy: Temporal scales, structure spacing and terrain effects, Bound.-Lay. Meteorol., 122, 123–147, 2007a.

Thomas, C. and Foken, T.: Flux contribution of coherent structures and its implications for the exchange of energy and matter in a tall spruce canopy, Bound.-Lay. Meteorol., 123, 317–337, 2007b.

Thomas, C., Mayer, J.-C., Meixner, F. X., and Foken, T.: Analysis of the low-frequency turbulence above tall vegetation using a Doppler sodar, Bound.-Lay. Meteorol., 119, 563–587, 2006.

Thomas, R. M., Trebs, I., Otjes, R., Jongejan, P. A. C., Brink, H. T., Phillips, G., Kortner, M., Meixner, F. X., and Nemitz, E.: An automated analyzer to measure aurface-atmosphere exchange fluxes of water soluble inorganic aerosol compounds and reactive trace gases., Environ. Sci. Technol., 43, 1412–1418,

doi:10.1021/es8019403, 2009.

Trebs, I., Meixner, F. X., Slanina, J., Otjes, R., Jongejan, P., and Andreae, M. O.: Real-time measurements of ammonia, acidic trace gases and water-soluble inorganic aerosol species at a rural site in the Amazon Basin, Atmos. Chem. Phys., 4, 967–987, doi:10.5194/acp-4-967-2004, 2004.

Verhoef, A., McNaughton, K. G., and Jacobs, A. F. G.: A parameterization of momentum roughness length and displacement height for a wide range of canopy densities, Hydrol. Earth Syst. Sci., 1, 81–91, doi:10.5194/hess-1-81-1997, 1997.

Vogel, H.-J. and Roth, K.: Moving through scales of flow and transport in soil, J. Hydrol., 272, 95–106, 2003.

Wichura, B.: Untersuchung zum Kohlendioxid-Austaisch über einem Fichtenwaldbestand, Hyperbolic-Relaxed-Eddy-Accumulation Messungen für das stabile Kohlenstoffisotop ^{13}C und Waveletanalysen des turbulenten Kohlendioxid-Austauschs, Bayreuther Forum Ökologie, 114, 297 pp., 2009.

Wichura, B., Ruppert, J., Delany, A. C., Buchmann, N., and Foken, T.: Structure of carbon dioxide exchange processes above a spruce Forest, in: Biogeochemistry of Forested Catchments in a Changing Enivironment, A German Gase Study. Ecological Studies, edited by: Matzner, E., Ecological Studies, Springer, Berlin, Heidelberg, 161–176, 2004.

Wilczak, J. M., Oncley, S. P., and Stage, S. A.: Sonic anemometer tilt correction algorithms, Bound.-Lay. Meteorol., 99, 127–150, 2001.

Wolfe, G. M., Thornton, J. A., Bouvier-Brown, N. C., Goldstein, A. H., Park, J.-H., McKay, M., Matross, D. M., Mao, J., Brune, W. H., LaFranchi, B. W., Browne, E. C., Min, K.-E., Wooldridge, P. J., Cohen, R. C., Crounse, J. D., Faloona, I. C., Gilman, J. B., Kuster, W. C., de Gouw, J. A., Huisman, A., and Keutsch, F. N.: The Chemistry of Atmosphere-Forest Exchange (CAFE) Model – Part 2: Application to BEARPEX-2007 observations, Atmos. Chem. Phys., 11, 1269–1294, doi:10.5194/acp-11-1269-2011, 2011a.

Wolfe, G. M., Thornton, J. A., McKay, M., and Goldstein, A. H.: Forest-atmosphere exchange of ozone: sensitivity to very reactive biogenic VOC emissions and implications for in-canopy photochemistry, Atmos. Chem. Phys., 11, 7875–7891, doi:10.5194/acp-11-7875-2011, 2011b.

Wolff, V., Trebs, I., Ammann, C., and Meixner, F. X.: Aerodynamic gradient measurements of the NH_3-HNO_3-NH_4NO_3 triad using a wet chemical instrument: an analysis of precision requirements and flux errors, Atmos. Meas. Tech., 3, 187–208, doi:10.5194/amt-3-187-2010, 2010.